# AN EXPERIMENTAL INVESTIGATION OF FLAME PROPAGATION DOWNSTREAM OF A CYLINDRICAL FLAMEHOLDER

ROBERT SCOTT SATRE

# AN EXPERIMENTAL INVESTIGATION OF FLAME PROPAGATION DOWNSTREAM OF A CYLINDRICAL FLAMEHOLDER

Thesis by

Robert Scott Satre II

Lieutenant, United States Navy

In Partial Fulfillment of the Requirements

For the Degree of

Aeronautical Engineer

California Institute of Technology

Pasadena, California

1959

ACKNOWLEDGMENT

I am deeply grateful to Dr. Edward E. Zukoski for suggesting this thesis topic and giving so freely of his time and efforts in bringing it to completion. His enthusiastic support made the entire project a very pleasant experience.

Sincere thanks are due to Dr. F. H. Wright of the Jet Propulsion Laboratory for his many helpful suggestions in the conduct of the experiments and comments on this manuscript. I would also like to thank the laboratory personnel, and in particular Mr. Davis Ragan, for their efforts in maintaining and operating the experimental equipment.

The excellent work of Miss Helen Burrus in preparing the manuscript and Mrs. Betty Wood in preparing of the figures is also deeply appreciated.

## ABSTRACT

Flame propagation downstream of a 1/8 inch circular cylindric flameholder was studied experimentally. The effects on flame spreading of the fuel-air mixture velocity and such chemical parameters as fuel-air ratio, mixture temperature, and fuel composition were determined. Combustion wake widths were determined from measurement of spark Schlieren photographs.

The data indicate that flow was laminar up to a critical velocity corresponding to a Reynolds number of $0.9 \times 10^4$, and turbulent for super critical velocities. The experiments were restricted to the turbulent flow regime. In this regime, the wake width was velocity independent and fuel-air ratio had only a slight effect. There was a small, and nearly linear, decrease in wake width as the temperature was increased. The effect of substitution of hydrogen gas for hydrocarbon fuel revealed that turbulent wake spreading was independent of fuel composition.

Comparison of the experimental results with theoretical treatments of flame spreading showed that none of the existing theories was satisfactory.

TABLE OF CONTENTS

# LIST OF TABLES

LIST OF FIGURES

LIST OF FIGURES (cont'd)

## LIST OF SYMBOLS

| | |
|---|---|
| $f$ | fraction of fuel-air mixture burned |
| $s$ | average flame speed |
| $U_o$ | approach stream velocity |
| $x$ | distance downstream of flameholder |
| $H$ | combustion chamber half height |
| $\lambda$ | ratio of density of unburned gas to density of burned gas |
| $\phi$ | fuel-air equivalent ratio, fraction of stoichiometric |
| $\Delta P_T$ | loss of total pressure in combustion chamber |
| $q$ | dynamic pressure |

# INTRODUCTION

Supersonic jet aircraft are all powered by afterburning turbojet engines, and several present day air breathing guided missiles utilize ram jet engines. Both the ram jet and the afterburner require continuous burning of a very hign velocity combustible mixture. The mixture velocities in these engines are considerably higher than the flame speeds of any fuels currently used; hence, a method of maintaining combustion must be devised. This problem has been successfully solved by placing bluff bodies of various shapes and sizes in the path of the combustible mixture. The recirculating gases in the wake of the bluff body provide a continuous source of ignition for the fast moving fuel-air mixture.

The experimental work of Nicholson and Fields (Ref. 1), Longwell (Ref. 2), Scurlock (Ref. 3), and Haddock (Ref. 4) showed that it was indeed possible to stabilize a flame at very high mixture velocities by use of bluff body flameholders. Figure 1 illustrates the appearance of a bluff body stabilized flame. The flame can be divided into two distinct regions, the recirculation region immediately behind the flameholder, and the propagating flame extending downstream from the recirculation region. Zukoski (Ref. 5) divides the recirculation region into two zones, recirculation and mixing. The former zone consists solely of recirculating hot gases and the latter the region of mixing of recirculating gases with the unburnt mixture. It is in the mixing zone that ignition takes place. Here the burnt gases supply heat to the fuel-air mixture and initiate combustion. Ignition will be continuous provided there is sufficient heat transfer in this zone.

The flame propagating region is the one of interest in this report. There are many variables affecting the spreading rate of the flame in this region, and as yet there has been no satisfactory theoretical treatment of the spreading process. Thurston (Ref. 6) recently investigated some of the fluid dynamical parameters involved in flame spreading, including such things as combustion chamber length, upstream blockage, and flameholder size. The present work was undertaken to determine the effects of various chemical parameters on flame spreading. These parameters included fuel-air ratio, mixture temperature, and the chemical composition of the fuel.

The primary method of obtaining data was the measurement of flame width from spark Schlieren photographs. An average wake boundary was defined and used consistently throughout the investigation. As a supplement to the Schlieren measurements, wake widths were also determined from total pressure profiles taken at selected downstream stations.

## EXPERIMENTAL APPARATUS

General. A schematic diagram of the equipment used in this investigation is shown in figure 2. The apparatus includes the systems used for air supply and control, liquid fuel and hydrogen gas supply, and temperature and pressure measurements.

A regulated quantity of air was heated to the desired temperature in the heat exchanger. Fuel was then injected into the air stream well upstream of the plenum chamber to insure homogeneity of the fuel-air mixture. A smoothly converging nozzle connected the plenum chamber and the combustion chamber. The plenum chamber screens in conjunction with the convergent nozzle produced a uniform rectilinear flow of low turbulence level at the entrance to the combustion chamber.

Air Supply and Control System. Air was furnished by a compressor of 3.7 pounds per second capacity at a regulated pressure of 65 psig. Control of the mass flow rate of air was accomplished by a sonic throat regulating valve located upstream of the heat exchanger. Thus, changes in air temperature and fuel-air ratio had no effect on the mass flow rate of air supplied to the system.

Air Temperature Control. The air temperature was regulated by passing a portion of the air through a multitube heat exchanger. The heat exchanger utilized a turbojet can burner with a separate air supply as heat source. Two butterfly valves fixed the fraction of air which passed through the heat exchanger. These valves and the fuel pressure to the heat exchanger burner could be operated independently or in

concert to obtain the desired air temperature. This system allowed the air temperature to be controlled quite precisely, within $\pm 5^{\circ}$ F, for prolonged periods of time regardless of changes made in the mass flow rate of air and/or fuel-air ratio. Mixture temperatures which were used ranged from $100^{\circ}$ F to $465^{\circ}$ F; the latter was the maximum temperature that could be maintained for long periods of time at high mass flow rates.

Fuel System. The liquid fuel used was Standard Oil Thinner No. 200, which is described in detail in Table A. This fuel was chosen because of its ready availability, uniformity, and ease of handling and metering. The fuel tanks were pressurized to 150 psig with bottled nitrogen. The fuel was metered through a Fisher Porter Flowrater, which could be read to within $\pm$ 1/2 pound per hour, and then injected into the air stream well upstream of the plenum chamber. This allowed ample time for complete fuel vaporization and mixing with the air.

The hydrogen gas, supplied from a bank of 20 hydrogen bottles, was passed through another flowrater and was then injected into the air stream at the same point as the liquid fuel. Four nitrogen bottles were used in this system to purge all fuel lines before and after all experiments.

The fuel system thus allowed any desired combination of liquid fuel and hydrogen gas to be used.

Ignition System. Ignition of the fuel-air mixture was accomplished by a high voltage spark between a movable ignition wire and the flameholder. The power supply of 10,000 volts provided a spark, across a

gap of approximately 1/4 inch, which produced ignition of a stoichiometric mixture at flow velocities of up to 200 feet per second. When hydrogen gas was used as fuel, ignition could be accomplished at even higher flow velocities.

Plenum Chamber and Nozzle. The plenum chamber was a 5 foot long circular cylinder 15 inches in diameter. Six 150 mesh wire screens were mounted in the plenum chamber to reduce the turbulence level of the mixture. As a safety measure, a 10 inch blowout disk was located at the rear of the plenum chamber and a flame arrestor was placed slightly upstream of the chamber to prevent flashback through the lines.

The 18 inch long nozzle was contoured smoothly from a 15 inch diameter to the 1 by 4 inch rectangular cross section of the combustion chamber. This arrangement produced a flat velocity profile at the entrance to the combustion chamber.

Combustion Chamber and Flameholder. The combustion chamber was a rectangular duct 15 inches long with a 1 by 4 inch cross section; a view of the chamber is shown in figure 3. The side walls were made up of two 6 inch wide Vycor glass plates divided in the center and supported at the ends by 1 inch wide water cooled steel plates. This allowed sufficient cooling to prevent warping of the duct and cracking of the glass plates. The forward steel strip also served as a mounting plate for the 1/8 inch flameholder. The flameholder was mounted 1/4 inch upstream of the Vycor glass and midway between the top and bottom walls of the duct. The glass walls allowed visual and photo-

graphic observations of the spreading flow to be made. The glass and metal strips were spaced close enough that no disturbances were produced in the combustion chamber by outflow of gas.

A 1/8 inch water cooled flameholder was used exclusively for the conduct of experiments. Cold flow was investigated by utilizing a hollow 1/8 inch cylinder which was blocked at one end and connected to a helium bottle through a pressure reduction valve at the other. The helium was injected to produce a sufficient density gradient for the taking of Schlieren pictures. Five holes of 0.013 inch diameter were drilled in the cylinder at 0.2 inch intervals, and helium under 30 psig pressure was fed into the cylinder. A flat copper splitter plate was soft soldered to the cylinder to prevent the formation of an asymmetric Kármán vortex street. The plate was 1 1/2 inches long and had a 0.15 inch cutout next to the cylinder to allow spreading of the helium.

Schlieren System. The Schlieren system was a double mirror type, and two 6 inch diameter mirrors with 48 inch focal length were used. A BH-6 mercury light source was used when conducting experiments with liquid fuel. The spark duration was approximately 10 microseconds. The light flash and the camera were synchronized to furnish the time delay necessary between shutter opening and spark flash. A shorter duration spark was needed when Schlieren photographs of the hydrogen flame were taken, and a spark source of approximately 2 microsecond duration was then substituted for the BH-6 lamp. The spark source was also used in taking photographs of the cold flow.

Pressure and Temperature Measurements. Plenum chamber pressure and combustion chamber static pressure were measured by water and mercury manometers. The pressure tap for the plenum chamber was approximately 2 feet upstream of the flameholder. A series of static pressure taps 1 inch upstream of the flameholder were fed into a common line to get an average static pressure at the combustion chamber entrance. A standard U-tube manometer was used for total pressure wake surveys and static pressure readings downstream of the flameholder.

Total pressure surveys were made at stations 2.6, 7.7, and 11.7 inches downstream of the flameholder, at mixture temperatures of 165° F and 465° F, at the same Mach number, and with a stoichiometric fuel-air ratio. A water cooled total pressure probe was used, and it was mounted so as to permit both vertical and fore and aft movement. The tip of the probe was 1/16 inch in diameter and extended about 1 inch beyond the water cooled jacket. The vertical position of the probe could be estimated within $\pm$ 0.05 inches and the position downstream of the flameholder within $\pm$ 0.10 inches. The turbulence of the flame front and the heating of the probe caused some wandering of the probe in the duct. Hence it was necessary to repeat all measurements at least twice as a check on the experimental accuracy. The same equipment was used to obtain cold flow total pressure profiles and static pressure measurements in the duct. Only the probe tip was replaced for the latter measurements.

Temperatures were measured by use of a chromel-alumel thermocouple located in the plenum chamber, and a Brown Automatic Potentiometer was used to read the thermocouple voltage.

## EXPERIMENTAL PROCEDURE

Schlieren Photographs. The principal source of data for this report was the measurement of wake widths from spark Schlieren photographs. All wake widths of burnt gases were determined from traces of these photographs, which were taken at 1:1 scale. A steel scale 4.002 inches long and 2.007 inches high was physically attached to the side wall of the duct, and the Schlieren system then moved about until the scale appeared in the ground glass screen of the camera at its actual size.

Figure 4 shows that the edge of the wake of the burnt gases consists of a series of small waves. These waves move downstream with the same velocity as the unburnt gas, and a spark duration of less than 10 microseconds was necessary to produce clearly detailed photographs. To determine an average wake width at any given downstream station, several photographs were taken under the same conditions and traces of these were then superimposed. The average wake width was then estimated by equating wave areas above and below the average boundary line as illustrated in figure 5. The scatter of data obtained by use of this technique was less than $\pm$ 0.04 inches. Measurements made from the same photographs after a considerable period of time indicated that the reproducibility of this technique was also within $\pm$ 0.04 inches.

Due to the small size of the Schlieren system mirrors, it was necessary to photograph the forward 6 inch section of the duct and then move the system back and repeat the procedure at the rear 6 inch section. In the interest of time saving, a complete series of tests was

made with the system set up at one station and then conditions were duplicated and photographs again taken at the other station. Duplication of flow conditions was easily accomplished. This arrangement made it necessary to omit the section of the duct between 5 and 8 inches downstream of the flameholder in the two sets of photographs.

Downstream Blockage. In conducting these experiments it was necessary to choose operating conditions such that there were no strong acoustic oscillations in the combustion chamber. The effects of these oscillations is illustrated by one of the preliminary experiments which was conducted in an attempt to determine the effect of downstream blockage on flame spreading. The upper and lower surfaces of the duct were sloped from a point 7 inches downstream of the flameholder to the duct exit with a change in duct height from 4 inches at the 7 inch station to 2.5 inches at the exit. The flame was pinched down at the exit and appeared as illustrated in figure 6. Slight oscillations of the flame were visible to the naked eye. The composite Schlieren photograph of figure 7 shows that there was indeed a strong oscillation present as a result of the area change. The waves were of very large amplitude and in some cases were completely disconnected.

The duct length and flameholder size were picked so that without downstream blockage stable operation with the hydrocarbon fuel was possible within the entire range of fuel-air ratios and velocities under consideration in this investigation. However, these oscillations did restrict the fuel-air and velocity ranges over which hydrogen fuel could be used.

# EXPERIMENTAL RESULTS

General Discussion. Typical views of a flame stabilized on a 1/8 inch circular cylinder are shown in the time exposure of figure 3 and the spark Schlieren photographs of figure 4. The general features of a burning wake in an enclosed duct will now be discussed with the aid of these photographs before proceeding to the detailed results.

The brightly illuminated regions of the time exposure photograph are the regions of active combustion in the wake. Hence, it is evident from figure 4 that the regions of active combustion form the boundaries of the wake. There are two such regions separated by a region of low luminosity and hence negligible chemical reaction. Independent temperature measurements in this region have shown that the gas here is indeed completely burnt and of uniform temperature. Near the flameholder the thick combustion zones merge and the central core disappears.

The Schlieren photographs reveal that the central core is a region of uniform density, in agreement with temperature measurements. The two combustion zones appear as regions of very strong density gradients, and it is evident that these regions are composed of a mixture of burnt, burning, and unburnt gases. The distinct wave structure of figure 4 is typical and did not vary appreciably with temperature or velocity. However, very near the blowoff limits the amplitude of the waves increased slightly.

The width of the wake for approximately the first 3 inches of travel downstream of the flameholder was independent of variations of any of the chosen parameters. The wake spreading in this region

was quite rapid and the effects of the variables under investigation were negligible in comparison with the fluid dynamical effects. Further downstream, in the flame propagation region, the wake spread less rapidly and the spreading here was found to depend slightly on the variables being investigated.

The velocity field outside the burning wake is fixed by the acceleration produced through heat addition in the wake. There is a monotonic decrease in pressure down the duct and a corresponding increase in the velocity of the unburnt gas. The burnt gas is also accelerated, and due to its lower density quickly reaches speeds greater than the unburnt material. This process is clearly indicated in figure 4. The waves of the boundary region incline downstream in the vicinity of the flameholder, and hence indicate that the unburnt gas has a higher velocity than the burnt gas. However, far downstream of the flameholder the inclination is reversed; this reversal shows that the hot gas now has the higher velocity.

This acceleration process produces a curvature of the streamlines in the unburnt gas. Hence, the spreading rate of the wake measured in this report was in part produced by the entrainment of material into the wake and in part by the curvature of the streamlines in the unburnt mixture.

Approach Stream Velocity. The effect of approach stream velocity on wake width is shown in figures 8, 9, 10, and 11. These figures show quite clearly that as the approach speed increased the wake width became progressively smaller in the flame propagation region. This

decrease in width continued until a critical velocity was reached; at velocities higher than critical, the wake width was independent of approach speed. The critical velocity at all temperatures and within the range of useful fuel-air ratios appeared to occur at the transition from laminar to turbulent flow, discussed by Zukoski and Marble (Ref. 7). This was plainly apparent in the Schlieren photographs. For example, in the velocity dependent region the wake was clearly laminar, with large smooth waves at the flame boundary. However, after transition a fine grained structure was superimposed on the waves, and the waves themselves were slightly smaller in amplitude but of about the same length.

To determine the transition Reynolds number, wake widths at the 12 inch station were plotted against Reynolds number for the four approach stream temperatures used. The data are presented in figure 12 with the widths normalized by the uniform value obtained at high velocity. The data indicate that a unique transition Reynolds number exists, and show that the value for transition, about $0.9 \times 10^4$, agrees very well with the optically determined value, $1.0 \times 10^4 \leq Re \leq 1.3 \times 10^4$, given in reference 5. It is evident that the two phenomena are identical and hence that the high velocity wake may properly be referred to as a turbulent flow.

Fuel-Air Ratio. Figures 13 and 14 illustrate the effect of fuel-air ratio on the wake growth. It is evident that for the conditions of figure 13, which is in the transition region, the wake width changed slightly with fuel-air ratio. The minimum width occurred at the stoichiometric fuel-air ratio; for example, the wake was about 15 per cent wider at

equivalence ratios of 0.8 and 1.2 than at the stoichiometric ratio at the 12 inch station. The situation was markedly different at speeds above the transition value. Figure 14 shows that there was little variation of wake width with fuel-air ratio for an operating speed above transition.

The nature of the dependence on fuel-air ratio is illustrated by the plot of wake width versus fuel-air ratio presented in figure 15. The data show that for speeds above the transition value, the lower curve of figure 15, the wake width was relatively independent of fuel-air ratio for most of the range, but that the width increased near the blowoff value by about 3 per cent. The upper curve of figure 15 illustrates a transition speed and indicates a maximum variation of about 7 per cent. The variation of wake width for speeds below transition steadily increased with distance downstream, figure 13, whereas the variation was constant for super transition speeds, figure 14.

These findings agree quite closely with the work of reference 6 in which is discussed the results of a similar investigation, which was carried out at considerably lower mixture temperatures and in a duct of different dimensions than was used in this investigation.

It is possible that a change in fuel-air ratio away from stoichiometric may cause an increase in the sensitivity of the wake to pressure oscillations, which could result in waves of larger amplitude and hence a wider wake. However, careful study of the Schlieren photographs showed no measurable change in the general character of the wake with fuel-air ratio variation. The mixture velocities above

the transition velocity are the velocities of practical interest, and here it is quite clearly shown that fuel-air ratio effects are negligible.

Temperature. The effect of variation of approach stream temperature on the wake was measured for temperatures ranging from 560° R to 925° R.

Examination of Schlieren photographs taken in the turbulent flow regime showed that the temperature had no systematic influence on the wave structure and the fine grained turbulence superimposed on the waves. Hence, it was expected that the principal effects of temperature variation would be the result of changes in density ratio and flame speed.

The measured variation of wake width with approach stream temperature is indicated in figures 8 to 11, from which the cross plot of figure 16 was obtained. The data of the latter figure are for the station 9 inches downstream of the flameholder and for Reynolds numbers above the critical value. The data show quite clearly that the wake width was nearly independent of approach stream temperature, and further that the observed variation was a small but definite decrease as the temperature was increased. This is a rather surprising result. For example, an increase in absolute temperature by a factor of 1.65 produced a decrease in wake width of about 12 per cent. For the temperature range investigated, the decrease of wake width was nearly linear with temperature increase.

The data of figure 16 are typical of similar cross plots obtained at other stations more than 4 inches downstream of the flameholder.

Within 4 inches of the flameholder wake width was found to be temperature independent. Farther downstream the per cent change in wake width corresponding to a given temperature change was nearly constant. This result is clearly illustrated in Table B, in which wake widths, normalized by the corresponding widths at 101° F, are presented for various stations downstream of the flameholder. The constant values of normalized widths shown in this table indicate that the wake width variation with temperature was not caused by any simple translation of the wake origin.

The effect of temperature, then, was a nearly linear decrease in wake width with increased temperature except near the flameholder, where there was no observed variation of width with temperature.

Fuel Chemistry. To determine the effect of the chemical composition of the fuel, and in particular of the flame speed, on wake width, several tests were made with varying ratios of hydrocarbon and hydrogen gas. Figure 17 shows profiles obtained with various mixtures of hydrogen and hydrocarbon fuels ranging from all hydrocarbon to all hydrogen. These data clearly show that the variation of fuel composition is unimportant in fixing wake width. The differences in the profiles of figure 17 are all well within the expected range of scatter of $\pm$ 0.04 inches.

The experiment was conducted in the turbulent flow regime, to assure that the fuel-air ratio would have a minimum effect upon the results. All runs were made at the same temperature and essentially the same flow velocity. It was not possible to use a stoichiometric

mixture when burning hydrogen alone because the system operated unstably when that fuel was used by itself. A study of the Schlieren photographs revealed that the combustion region of the wake had a finer grained structure superimposed on the waves when hydrogen was burned alone than when the hydrocarbon was burned alone. However, the waves could still be detected and were similar in appearance to those noted in other experiments.

It is evident that fuel composition is not an important parameter in the flame spreading process.

# DISCUSSION

Comparison of Theory and Experiment. Theoretical analyses of flame spreading from bluff bodies in a channel have been made in considerable detail by Scurlock (Ref. 8), Tsien (Ref. 9), and Iida (Ref. 10). These analyses were based on the assumptions of incompressible flow, an infinitesimally small flameholder, and a discontinuity in the flow field at the flame front. In addition these analyses were all based on the assumption of laminar flow. Recently Spalding (Ref. 11) presented a theoretical treatment for turbulent flow by use of an assumed similarity between the spreading wake and a turbulent jet.

The results of the analyses of references 8 through 11 are most often presented as a function of wake width versus the fraction of the flow burned. The variation between the curves predicted by these authors is negligible. In order to make a comparison between the present experimental determination of wake widths and the predicted values, it is necessary to extend these analyses to make it possible to compute wake widths in terms of distance downstream of the flameholder. This can be done in an approximate manner by assuming that the average flame propagation speed, $\overline{s}$, is constant along the flame front, and that the length of the flame front between the point of ignition and any downstream station, x, is the distance x. The latter assumption, though not exact because of the curvature of the flame front, introduces only a small error since the curvature is slight. Thus the fraction burned at any station x may be expressed as

$$f = \left(\frac{\overline{s}}{U_o}\right)\left(\frac{x}{H}\right)$$

where H is the duct half height, and $U_o$ the approach stream velocity. The dependence of wake width on fraction burned, f, is indicated in figure 18. The parameter $\lambda$ appearing on this figure is the ratio of the unburnt to burnt gas density. It is evident that the theory predicts a strong variation of wake width at any particular downstream station when either $\bar{s}/U_o$ or $\lambda$ is changed. The magnitude of these changes is shown in Table C for several general examples.

The first example corresponds to a variation of $U_o$; the second a variation of fuel-air ratio; the third a variation of approach stream temperature, and the fourth a change in fuel composition. The reference state for all examples is a station downstream of the flame-holder such that a wake width of 41 per cent is obtained when $\lambda = 8$, and $\phi = 1.0$. Fuel-air properties are evaluated for n-heptane from the data of reference 11, since this fuel is similar to the thinner used in the present work, and the values of flame speed etc. are not known for the thinner.

The last column of each table indicates the wake width corresponding to assumed upstream conditions predicted by theory at the reference station. The changes in the parameters illustrated in these tables all cause variations in wake width of sufficient magnitude to be measured experimentally. Comparison with the experimental data discussed in the previous section of this paper shows a complete lack of agreement for all cases, provided the flame is turbulent. The actual changes in wake width were of an opposite sense and were also not nearly as large as those predicted by theory. Therefore, it is evident that the theories of reference 8 through 10 are not satisfactory for turbulent flow.

The theory presented by Spalding was set up expressly for turbulent flame spreading and the spreading rate predicted by this theory depends only on the chemical properties of the fuel-air mixture through the variation of the density ratio, $\lambda$ . Comparison of this theory and the experimental data for wake width variation with $\lambda$ at a constant fuel-air ratio are given in Table D. Again there is no evidence of agreement between experiment and theory as regards the influence of $\lambda$ .

Pressure Fields. Analysis of the flow of a compressible gas through a flame front shows that the static pressure change across the flame is negligible in comparison with the static pressure and that the total pressure loss is given by $q(1 - \frac{1}{\lambda})$. Since $\lambda$ is generally between 4 and 8, the change in total pressure across the flame is of the order of the dynamic pressure.

Values of this change have been computed for conditions corresponding to those used in the experiments from which the total pressure data of figures 19, 20, and 21 were obtained. Experimental values of $\frac{\Delta P_T}{q}(1 - \frac{1}{\lambda})$ are compared with these calculated values in Table E. The values were taken at the center line of the 8 inch stations of figures 19 through 21, and q, which was 7 per cent higher than the value upstream of the flameholder, was evaluated at the flameholder position. The experimental losses were very nearly equal to the theoretically predicted losses, though slightly higher. Hence, it is evident that most of the losses were due to the combustion process. The difference between the experimental and theoretical

values is due to flameholder drag and viscous effects. Note that the variation of losses with $\lambda$ followed the predicted trend quite closely.

The dependence of total pressure loss on the dynamic pressure is also qualitatively correct. Thus in figures 19 through 21 the loss at the edge of the wake is seen to increase with distance downstream of the flameholder. This is as it should be, since the dynamic pressure increased in a similar manner.

Isothermal Flow. It was of interest to compare the isothermal pressure fields with those obtained for the burning wake. Schlieren photographs obtained with helium injected into wake revealed that the copper splitter plate effectively broke up the shed vorticity behind the flameholder and that the wake was very similar in appearance to the burning wake. However, the Schlieren photographs were too diffuse to allow wake width measurements to be made and it was necessary to make the total pressure measurements presented in figures 22 and 23 to determine the wake boundary accurately.

Figures 24 and 25 are cross plots of the wake widths versus downstream distance obtained from pressure measurements for the burning wake and isothermal wake respectively. The figures were plotted using 20 per cent of the pressure decrement as the reference level to define the wake boundary. It can be seen that the burning wake spreads at very nearly two and a half times the rate of the isothermal wake. This is to be expected because of the importance of the density ratio across the flame front and the loss of total pressure due to combustion in the hot wake. The spreading rate of the isothermal wake was found to agree quite closely with the results of Townsend (Ref. 12).

It is evident that wake spreading rates for hot flow and isothermal flow are not closely related and that the theory of isothermal wake spreading is not applicable to a burning wake. This is readily apparent in figure 26, where burning wake and cold flow total pressure profiles are shown.

# CONCLUSIONS

An investigation was undertaken to determine the effect of such chemical parameters as fuel-air ratio, mixture temperature and fuel composition on the spreading of a burning wake. The influence of approach stream velocity was also determined.

The variation of mixture temperature was found to have a small, but real, effect upon wake width. An increase in absolute temperature of the mixture by a factor of 1.65 resulted in a decrease of the wake width by approximately 12 per cent. This is a rather surprising result, since one would expect that an increase in mixture temperature would cause an increase in flame speed and hence, a large increase in wake width. The variation of wake width with temperature was found to be nearly linear over the range of temperatures investigated.

Fuel-air ratio had a decided effect upon wake width in the laminar flow regime; an increase of nearly 10 per cent over the stoichiometric width was found near the upper and lower blowoff limits. In the turbulent flow regime, operation with fuel-air ratios above and below stoichiometric also caused an increase in wake width, but the effect was found to be practically negligible. Again the variation was in the opposite sense from the expected variation and of much smaller amplitude.

The variation of fuel composition had a negligible effect upon wake spreading for the range of mixture ratios of hydrocarbon fuel and hydrogen gas covered. Evidently, wake spreading behind the

flameholder is completely independent of the chemical composition of the fuel used.

As mixture velocity was increased, the wake width became correspondingly smaller until a critical velocity, i.e. transition from laminar to turbulent flow, was reached. At higher velocities there was no dependence of wake width on velocity. It was found that this critical velocity corresponded to a Reynolds number of approximately $0.9 \times 10^4$.

Comparison of the experimentally determined values of wake width with present theoretical treatments of the problem revealed that none of the theories was satisfactory.

## REFERENCES


1. Nicholson, H. M., and Fields, J. P.: Some Experimental Techniques to Investigate the Mechanism of Flame Stabilization in the Wake of Bluff Bodies. Part I. Third Symposium on Combustion, Flame, and Explosion Phenomena, Baltimore, Williams and Wilkins Company, (1949), pp. 44-68.

2. Longwell, J. P., Cheveny, J. E., Clark, W. W., and Frost, E. E.: Flame Stabilization by Baffles in a High Velocity Gas Stream. Part I. Third Symposium on Combustion, Flame, and Explosion Phenomena, Baltimore, Williams and Wilkins Company, (1949), pp. 40-41.

3. Williams, G. C., Hottel, A. C., and Scurlock, A. C.: Flame Stabilization and Propagation in High Velocity Gas Streams. Part I. Third Symposium on Combustion, Flame, and Explosion Phenomena, Baltimore, Williams and Wilkins Company, (1949).

4. Haddock, G. W.: Flame-Blowoff Studies of Cylindrical Flameholders in Channeled Flow. Progress Report No. 3-24, Pasadena, Jet Propulsion Laboratory, (May 14, 1951).

5. Zukoski, E. E.: Flame Stabilization on Bluff Bodies at Low and Intermediate Reynolds Numbers. Thesis, California Institute of Technology, Pasadena, (June, 1954).

6. Thurston, D. W.: An Experimental Investigation of Flame Spreading from Bluff Body Flameholders. Thesis, California Institute of Technology, Pasadena, (June, 1958).

7. Zukoski, E. E. and Marble, F. E.: The Role of Wake Transition in the Process of Flame Stabilization on Bluff Bodies. Combustion Research and Review, Butterworth Press, (1955).

8. Scurlock, A. C.: Flame Stabilization and Propagation in High Velocity Gas Streams. Meteor Report No. 19, Cambridge, Massachusetts Institute of Technology, (May, 1948).

9. Tsien, H. S.: Influence of Flame Fronts on the Flow Field. Journal of Applied Mechanics, (1951), pp. 188-194.

10. Iida, H.: Combustion in Turbulent Gas Streams. Sixth Symposium (Int.) on Combustion. Williams and Wilkins Company, (1956), pp. 341-350.

11. Spalding, D. B.: Ends and Means in Flame Theory. Sixth Symposium (Int.) on Combustion. Williams and Wilkins Company, (1956), pp. 12-19.

12. Townsend, A. A.: The Structure of Turbulent Shear Flow. Cambridge Press, (1956), p. 135.

TABLE I

Properties of Standard Oil Thinner No. 200

| | | | |
|---|---|---|---|
| 1. | Heat of combustion, net | 18,675 BTU/lb. | |
| 2. | Average molecular weight | 96 | |
| 3. | Latent heat of vaporization at 77° F | 148 BTU/lb. | |
| | Vapor pressure at 100° F | 2.5 psi | |
| 4. | Density, specific at 60° F | 0.7366 | |
| | Density, lb./gal. at 60° F | 6.132 lb./gal. | |
| 5. | Hydrocarbon analysis | Saturates | 94.5 °/o |
| | | Olefins | 00.5 °/o |
| | | Aromatics | 5.0 °/o |
| 6. | Weight fractions | Carbon | 85.4 °/o |
| | | Hydrogen | 14.6 °/o |

TABLE B

WAKE WIDTH, NORMALIZED BY WAKE WIDTH AT 101° F MIXTURE TEMPERATURE, AT INDICATED DOWNSTREAM STATIONS

| | Wake Width at T / Wake Width at 101° F | | | |
|---|---|---|---|---|
| Distance Downstream | 101° F | 165° F | 300° F | 465° F |
| 2" | 1.00 | 0.99 | 0.97 | 0.94 |
| 4" | 1.00 | 0.98 | 0.94 | 0.90 |
| 9" | 1.00 | 0.98 | 0.93 | 0.89 |
| 12" | 1.00 | 0.98 | 0.92 | 0.89 |

# TABLE C

## EXAMPLES OF THEORETICALLY PREDICTED WAKE WIDTHS

1. Variation of Approach Velocity

| $\frac{u_o}{u_o \text{ reference}}$ | f | $\frac{\text{Wake Width}}{\text{Duct Height}}$ |
|---|---|---|
| 0.5 | 0.24 | 0.60 |
| 1.0 | 0.12 | 0.40 |
| 2.0 | 0.06 | 0.23 |

2. Variation of Fuel-Air Ratio

| $\phi$ | $\frac{u_o}{u_o \text{ reference}}$ | $\frac{\bar{s}}{\bar{s} \text{ reference}}$ | f | $\lambda$ | $\frac{\text{Wake Width}}{\text{Duct Height}}$ |
|---|---|---|---|---|---|
| 1.1 | 1.0 | 1.00 | 0.12 | 7.0 | 0.37 |
| 0.9 | 1.0 | 0.76 | 0.09 | 6.5 | 0.33 |
| 0.8 | 1.0 | 0.57 | 0.07 | 6.0 | 0.23 |

3. Variation of Temperature

| Temp $^oR$ | $\phi$ | $\frac{\bar{s}}{\bar{s} \text{ reference}}$ | f | $\lambda$ | $\frac{\text{Wake Width}}{\text{Duct Height}}$ |
|---|---|---|---|---|---|
| 560 | 1.0 | 1.00 | 0.12 | 7.7 | 0.40 |
| 610 | 1.0 | 1.24 | 0.15 | 6.8 | 0.45 |
| 925 | 1.0 | 2.22 | 0.27 | 4.4 | 0.56 |

TABLE C (cont'd)

EXAMPLES OF THEORETICALLY PREDICTED

WAKE WIDTHS

4. Variation of Fuel

| Fuel | $\phi$ | $\frac{\bar{s}}{\bar{s}\ \text{reference}}$ | f | $\lambda$ | $\frac{\text{Wake Width}}{\text{Duct Height}}$ |
|---|---|---|---|---|---|
| n-heptane | 0.7 | 0.5 | 0.06 | 5 | 0.19 |
| hydrogen | 0.6 | 1.0 | 0.12 | 5 | 0.34 |
| n-heptane | 1.0 | 1.0 | 0.12 | 8.0 | 0.41 |

# TABLE D

## COMPARISON OF THEORETICAL AND EXPERIMENTAL WAKE WIDTHS

**Variation of $\lambda$ with $\phi$:**

| Temp $^{o}R$ | $\phi$ | $\lambda$ | Experimental Wake Width / Duct Height | Theoretical (Spalding) Wake Width / Duct Height |
|---|---|---|---|---|
| 610 | 1.05 | 6.8 | 0.40 | 0.40 |
| 610 | 0.70 | 5.8 | 0.42 | 0.33 |

**Variation of $\lambda$ at constant $\phi$**

| Theory | | Experiment | | |
|---|---|---|---|---|
| $\lambda$ | Wake Width / Duct Height | Temp $^{o}F$ | $\lambda$ | Wake Width / Duct Height |
| 4.0 | 0.13 | 46.5 | 5.0 | 0.39 |
| 6.0 | 0.26 | 100 | 7.7 | 0.40 |
| 8.0 | 0.40 | — | — | — |

TABLE E

COMPARISON OF THEORETICAL AND EXPERIMENTAL VALUES OF $\frac{\Delta P_T}{q}$

| Temp $^{o}R$ | $\lambda$ | $\frac{\Delta P_T}{q_1}$(Theor.) | $\frac{\Delta P_T}{q_1}$(Exper.) |
|---|---|---|---|
| 630 | 6.8 | 0.86 | 0.98 |
| 925 | 5.1 | 0.795 | 0.91 |

Note: $q_o = \frac{1}{2} \rho_o u_o^2$ Data show $\frac{u_o}{u_1} = 1.07$

Thus $q_1 = 1.14\, q_o$

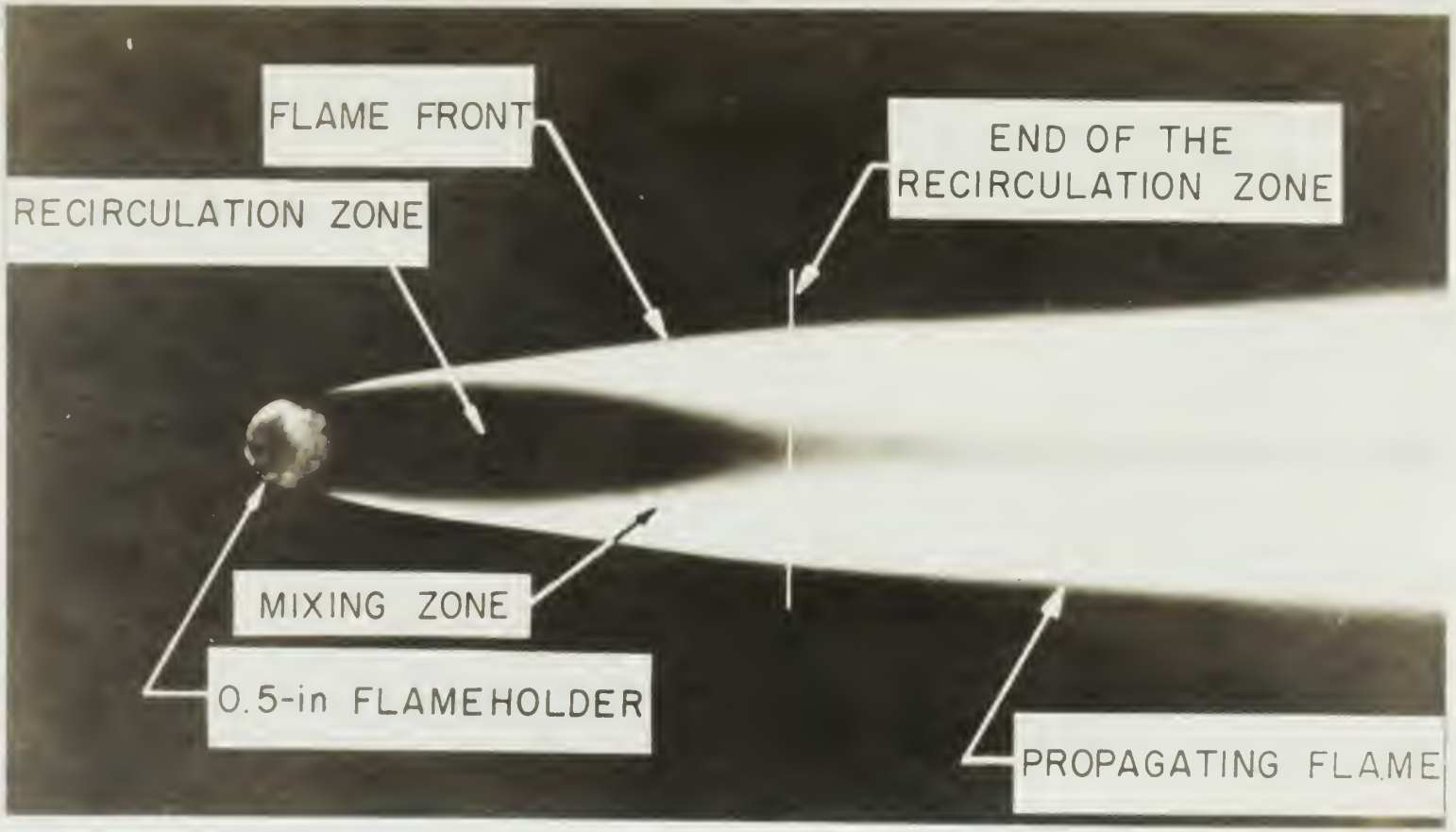


Fig. 1. Time exposure picture of flame stabilized on cylindric flameholder.

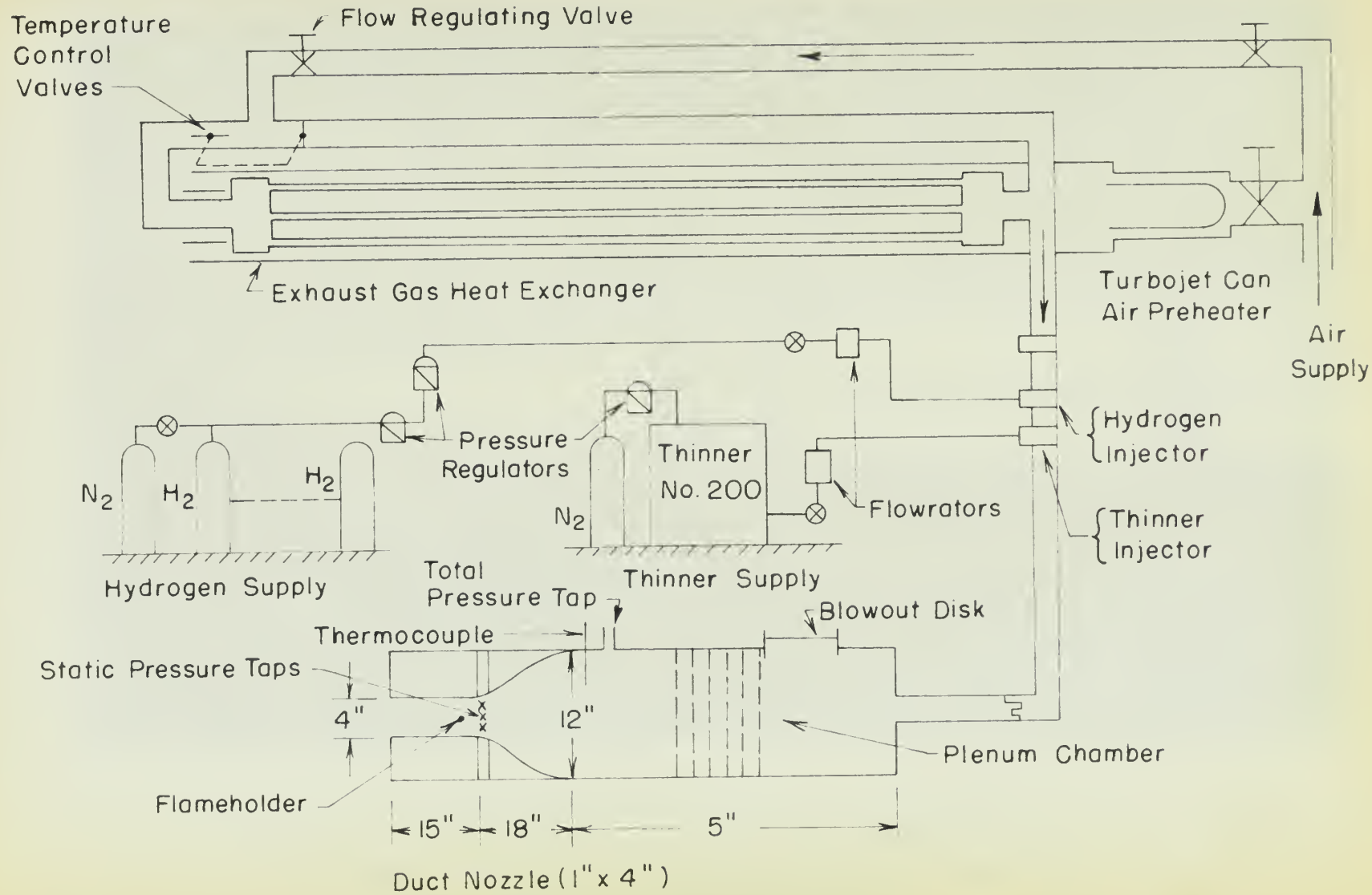


FIG. 2 – SCHEMATIC DIAGRAM OF EXPERIMENTAL APPARATUS

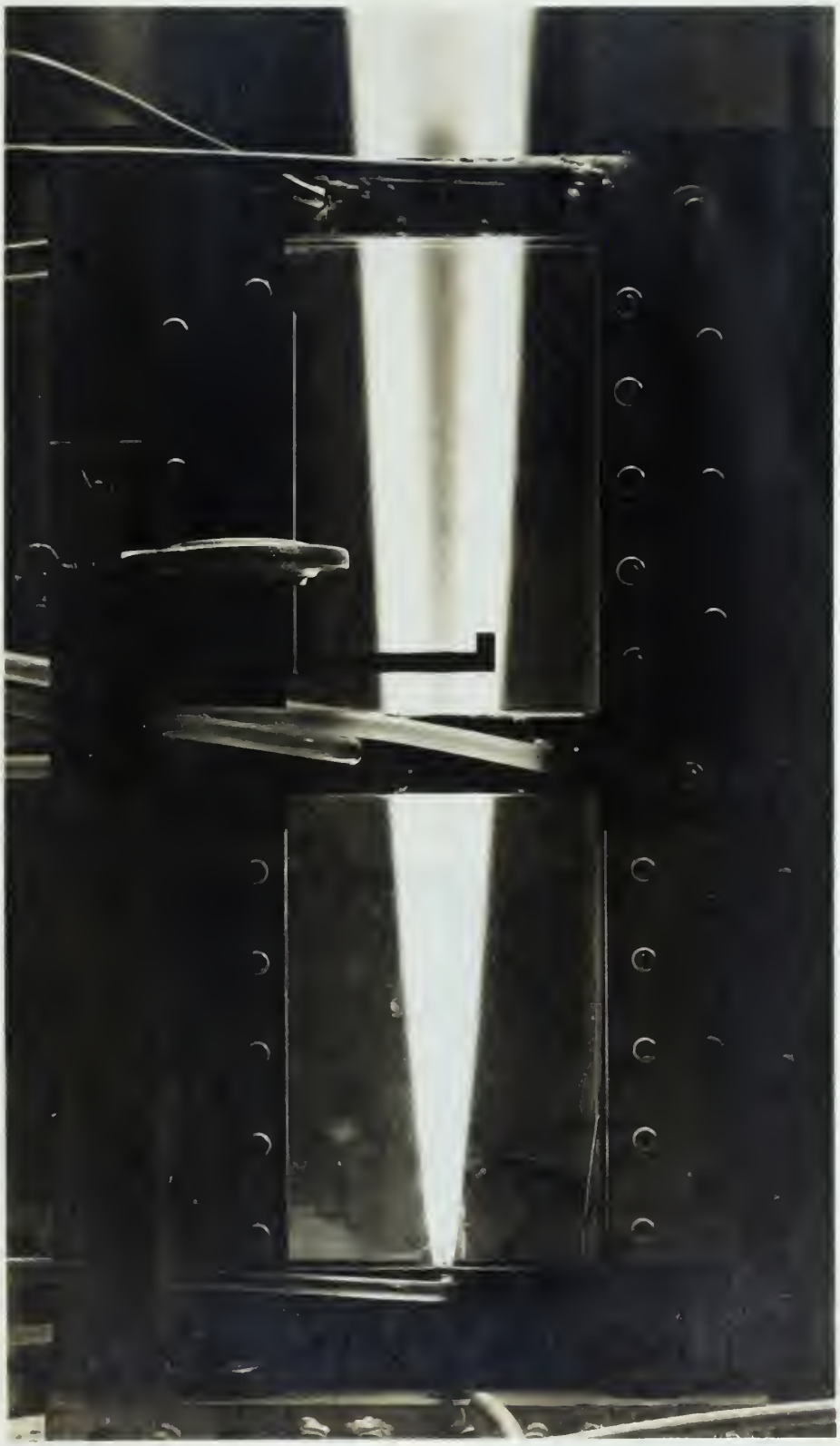

Fig. 3. Side view of combustion chamber showing flame stabilized on 1/8 inch flameholder.

Fig. 4. Composite Schlieren photograph of flame stabilized by 1/8 inch flameholder. $\phi = 1.0$. Velocity = 275 ft./sec.

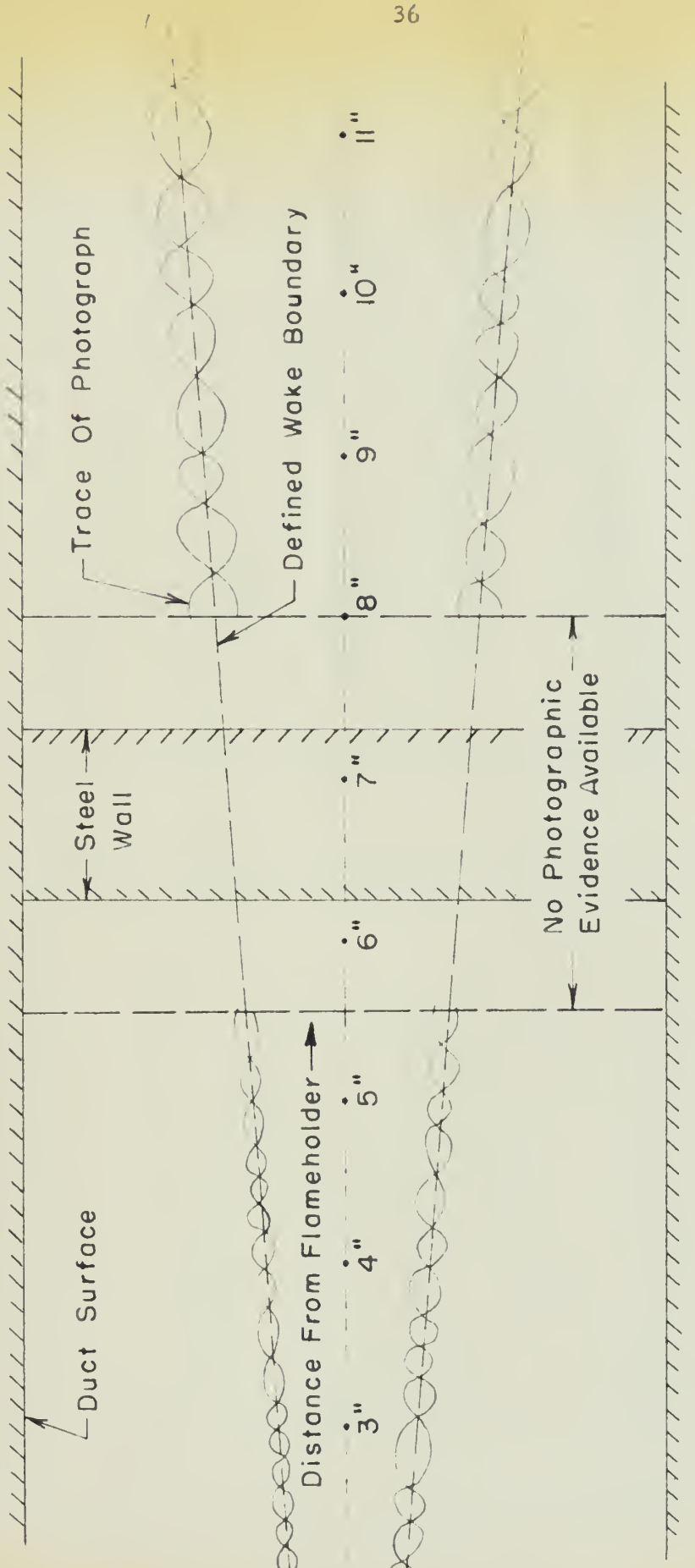


FIG. 5 – ILLUSTRATION OF BOUNDARY USED IN THE DETERMINATION OF WAKE WIDTHS

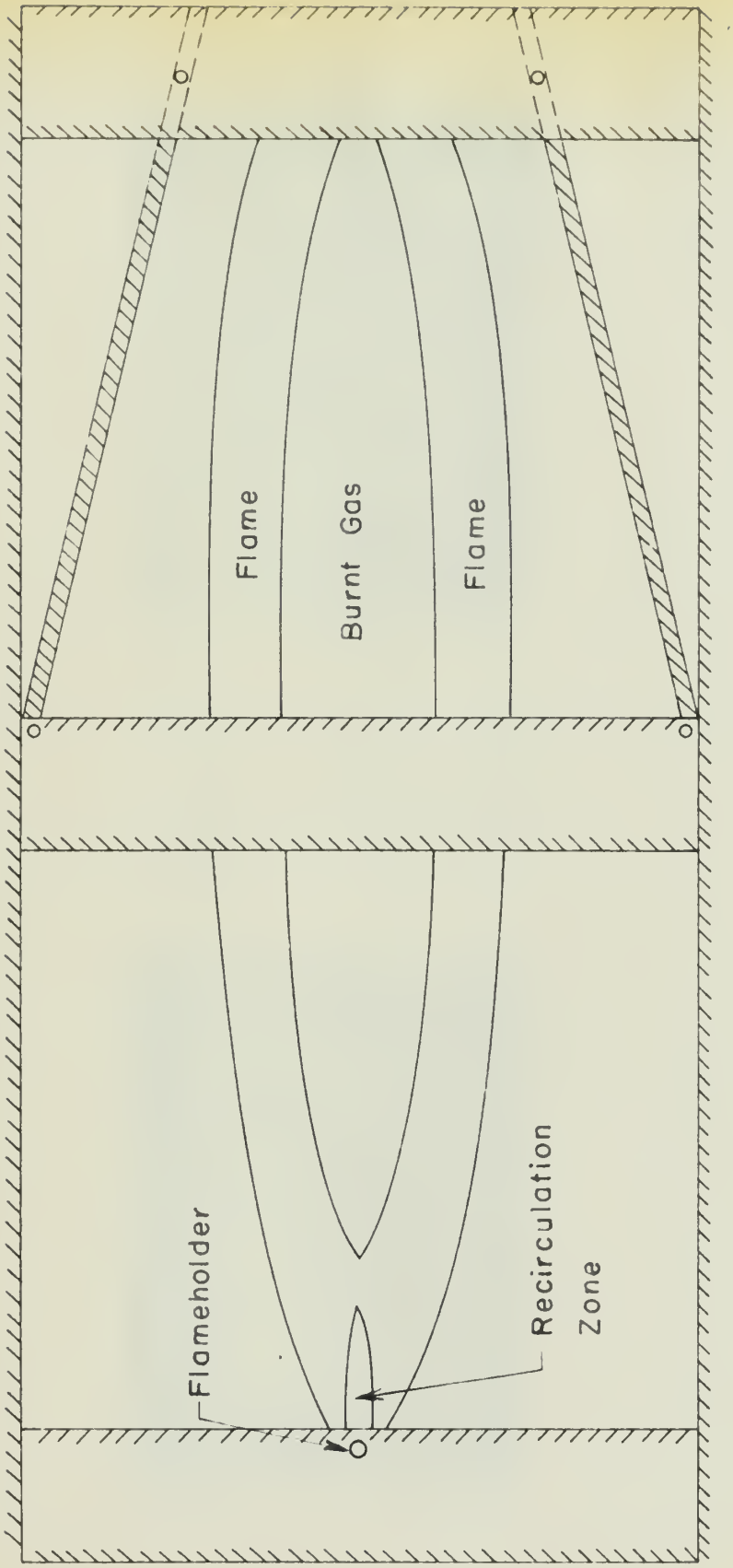


FIG. 6 – ILLUSTRATION OF PINCHING OF FLAME BY DOWNSTREAM BLOCKAGE OF THE DUCT

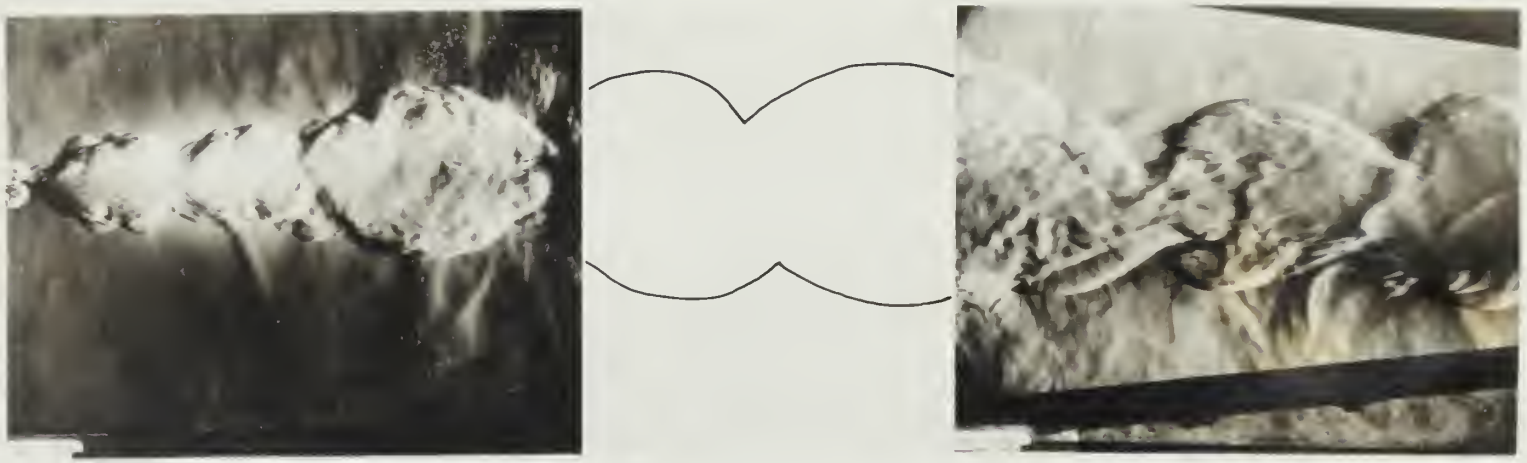

Fig. 7. Composite Schlieren photograph showing instability of flame caused by downstream blockage. $\phi = 1.0$. Velocity = 150 ft./sec.

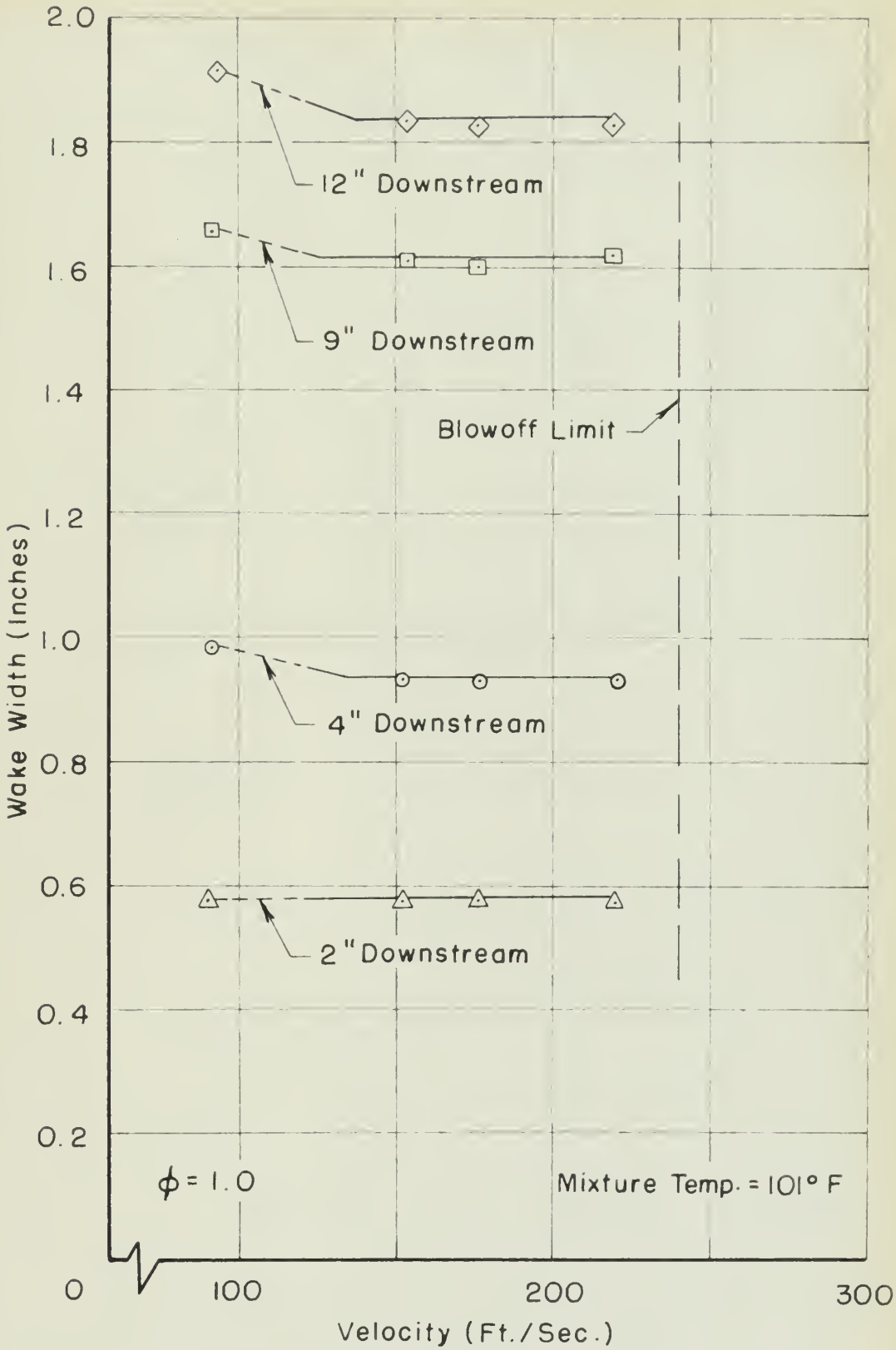


FIG. 8 - WAKE WIDTH AS A FUNCTION OF VELOCITY

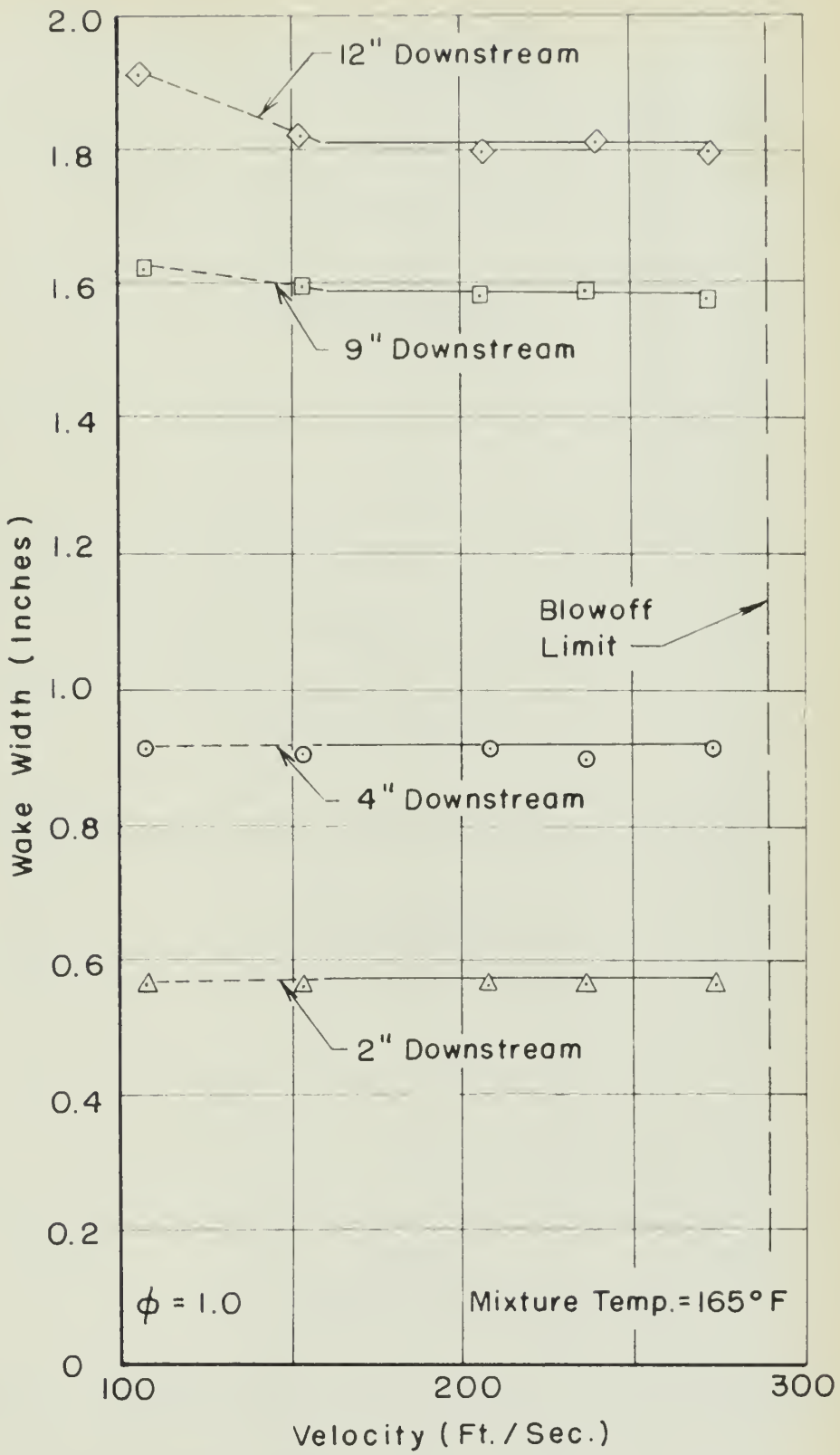


FIG. 9 – WAKE WIDTH AS A FUNCTION OF VELOCITY

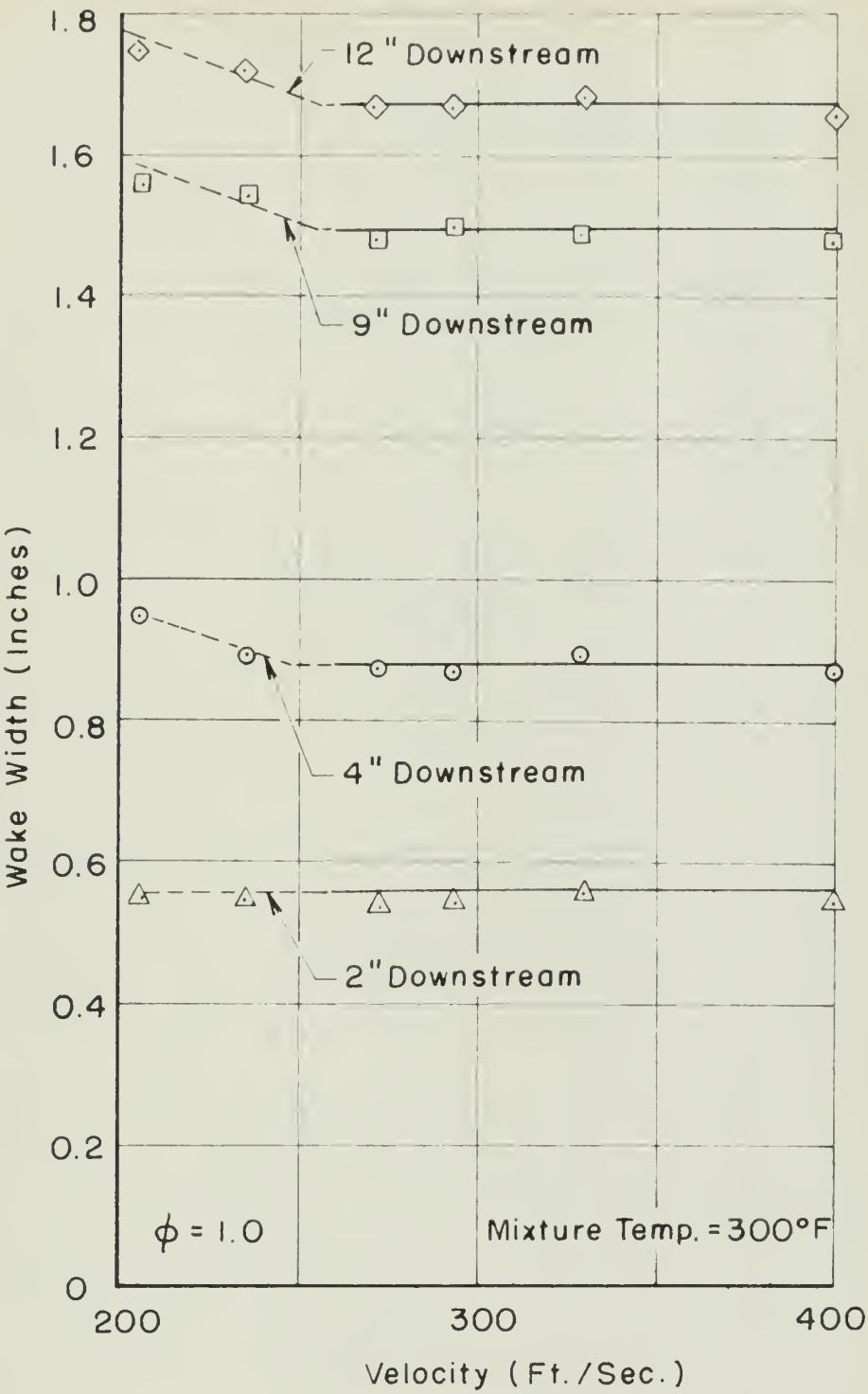


FIG. 10 - WAKE WIDTH AS A FUNCTION OF VELOCITY

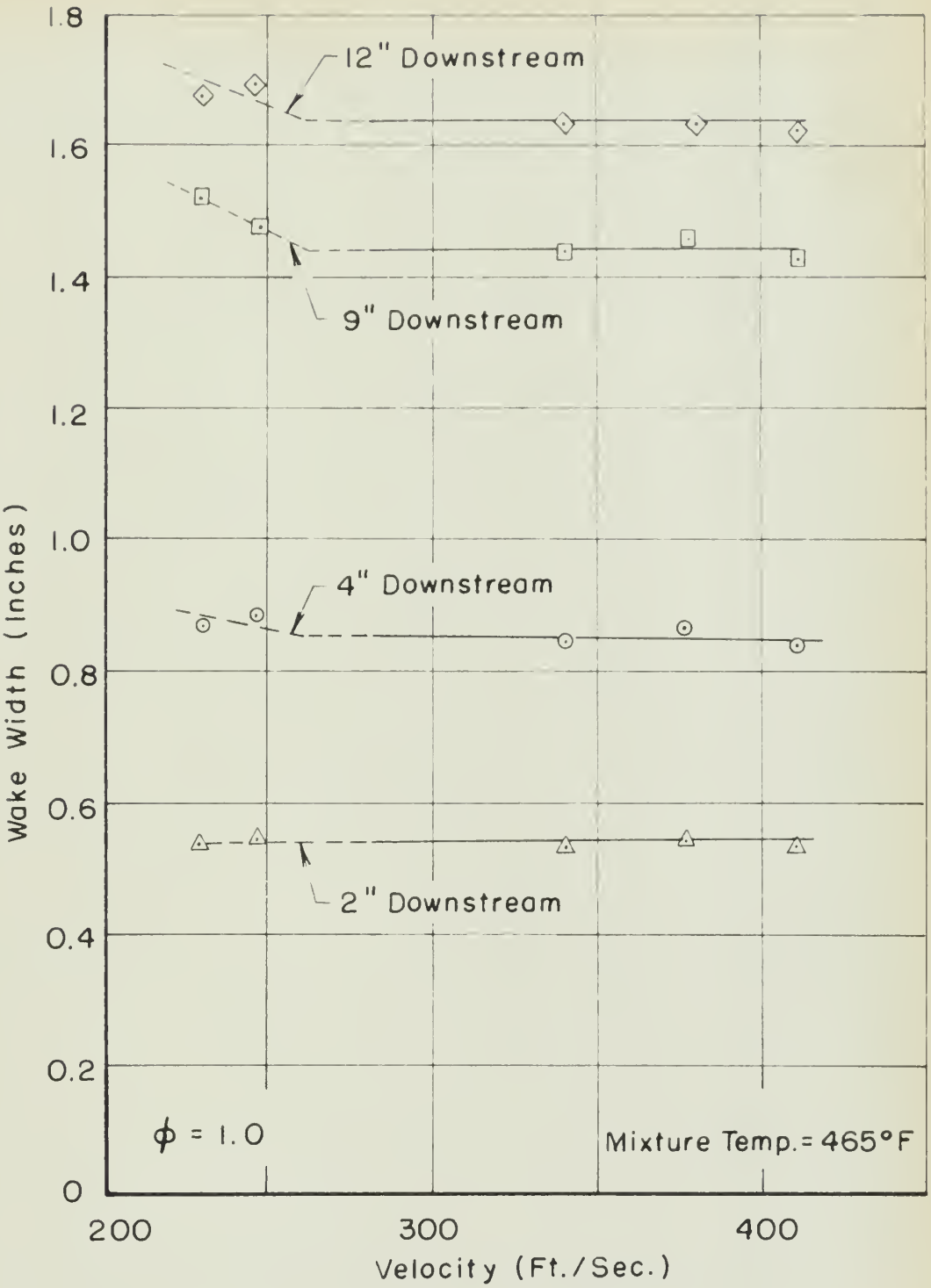


FIG. II – WAKE WIDTH AS A FUNCTION OF VELOCITY

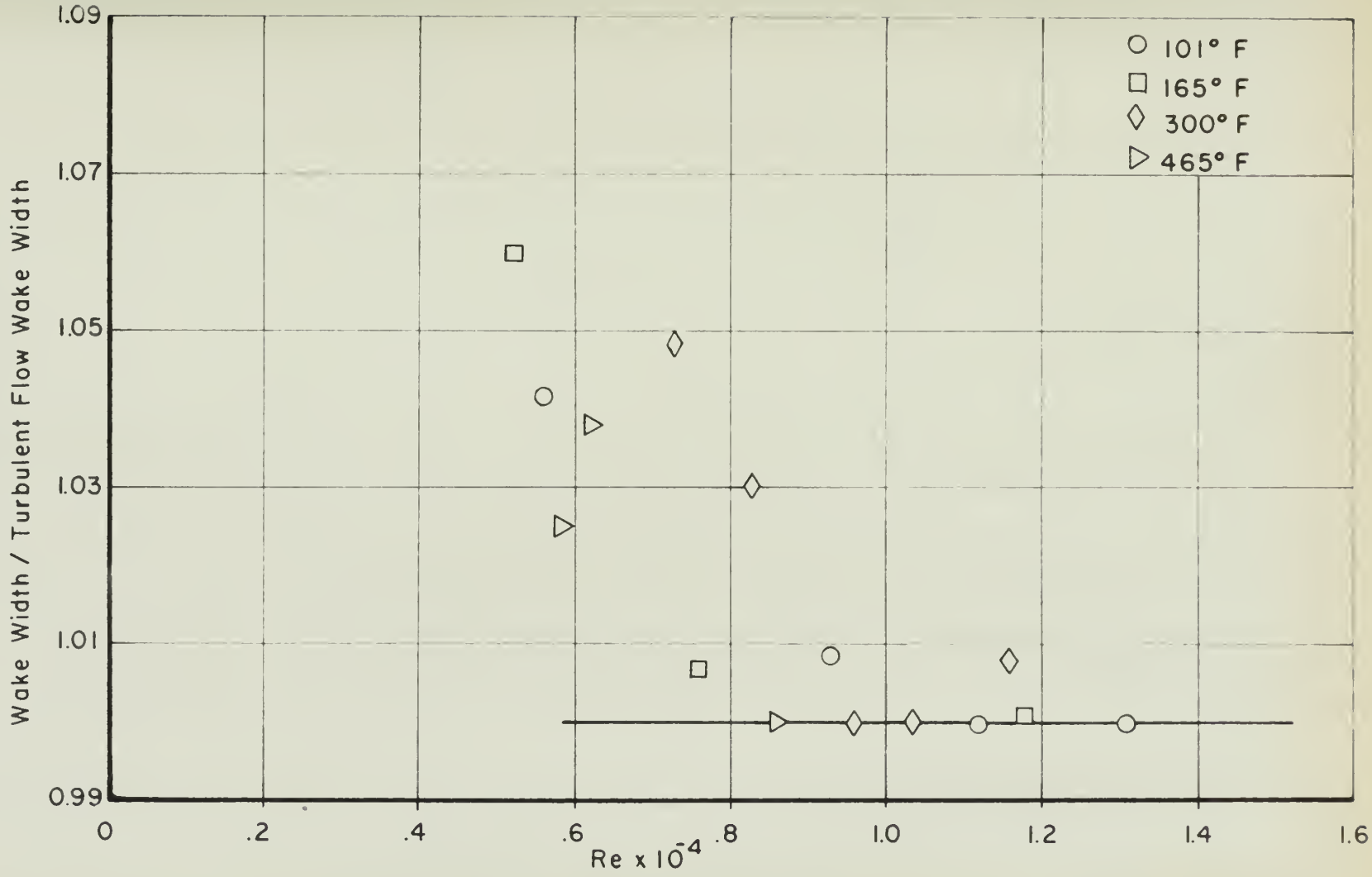


FIG. 12 – NORMALIZED WAKE WIDTH AS A FUNCTION OF REYNOLDS NUMBER

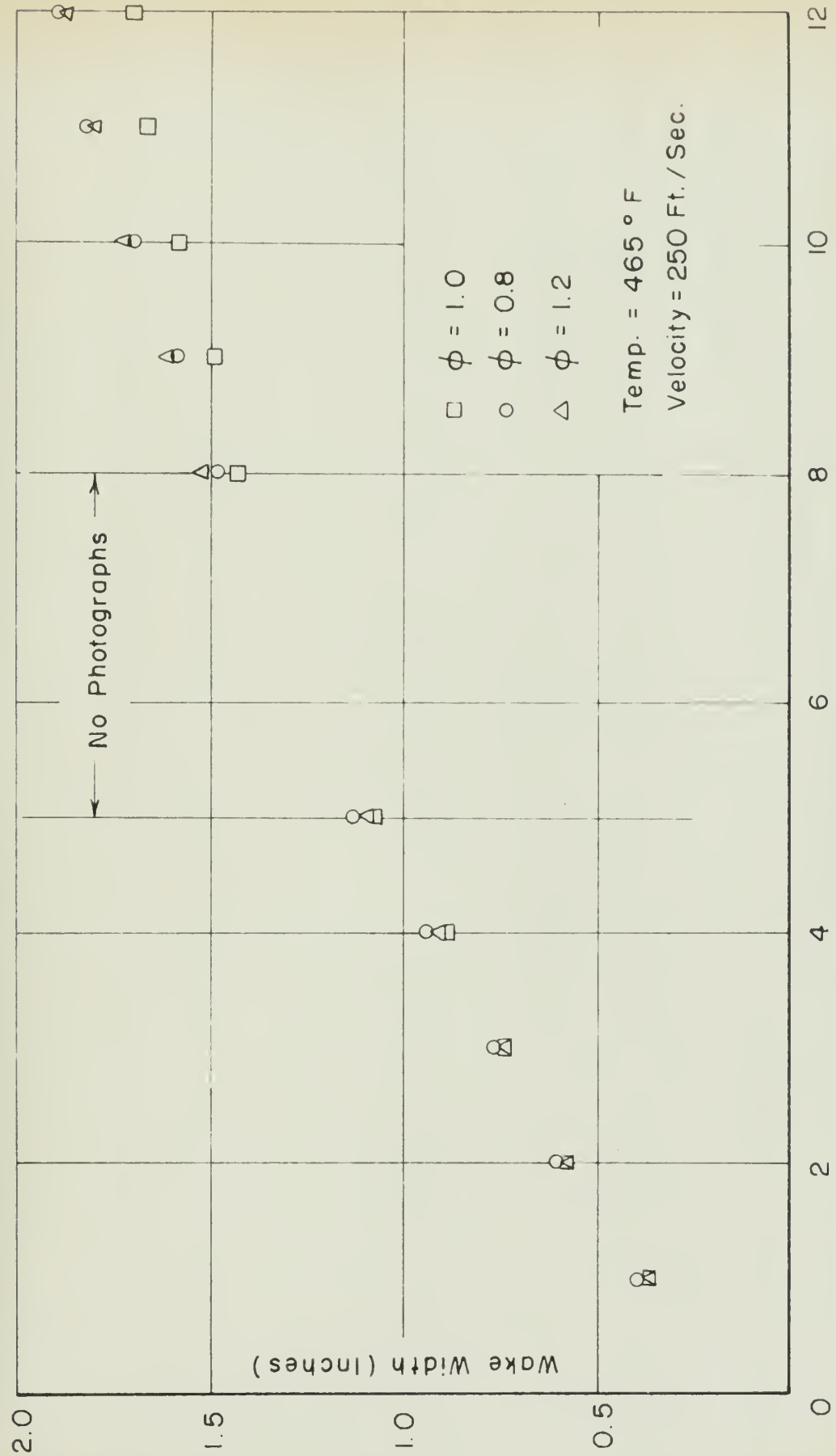


FIG. 13 - VARIATION OF WAKE WIDTH WITH FUEL-AIR RATIO - LAMINAR FLOW

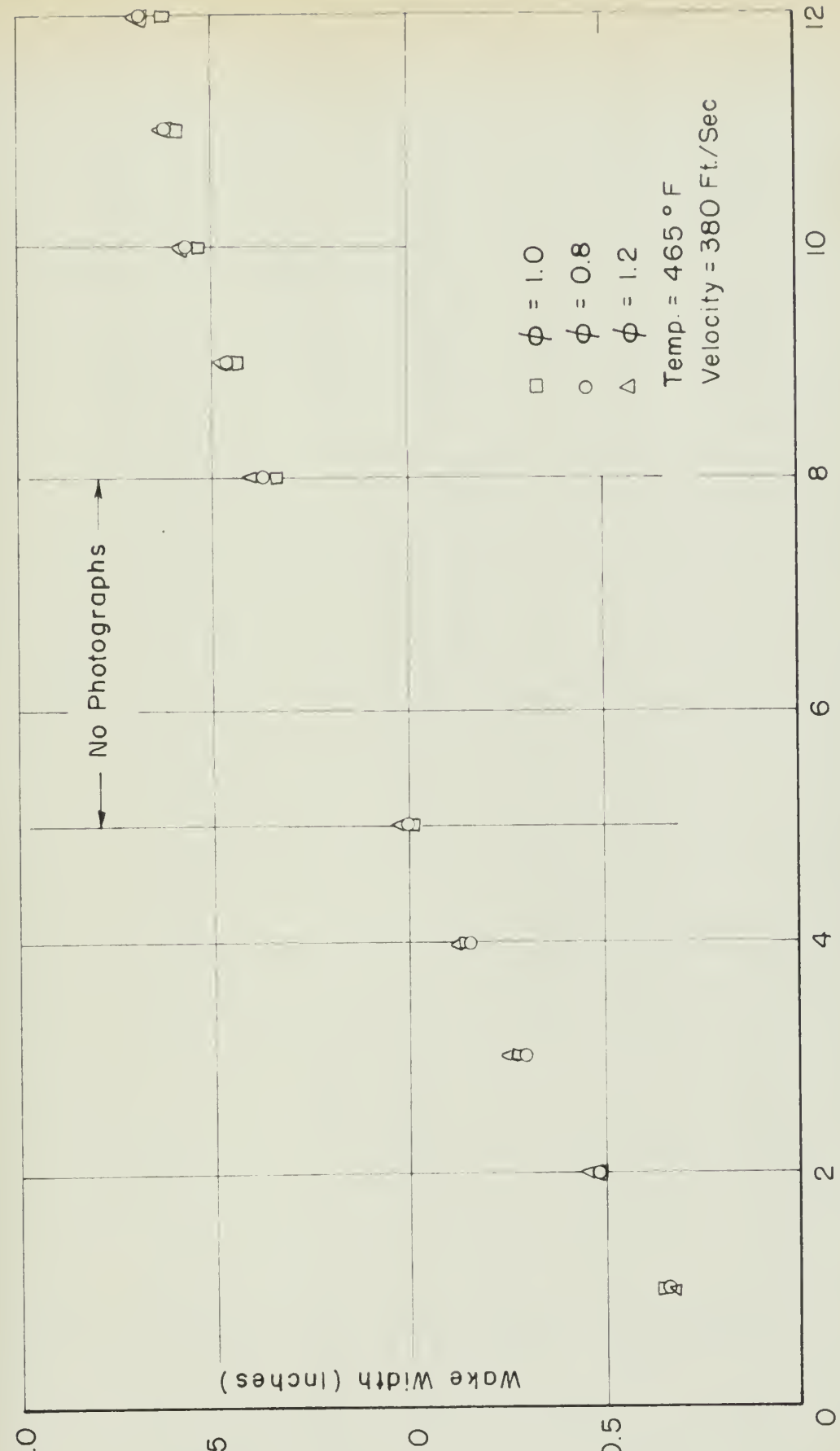


FIG. 14 - VARIATION OF WAKE WIDTH WITH FUEL - AIR RATIO - TURBULENT FLOW

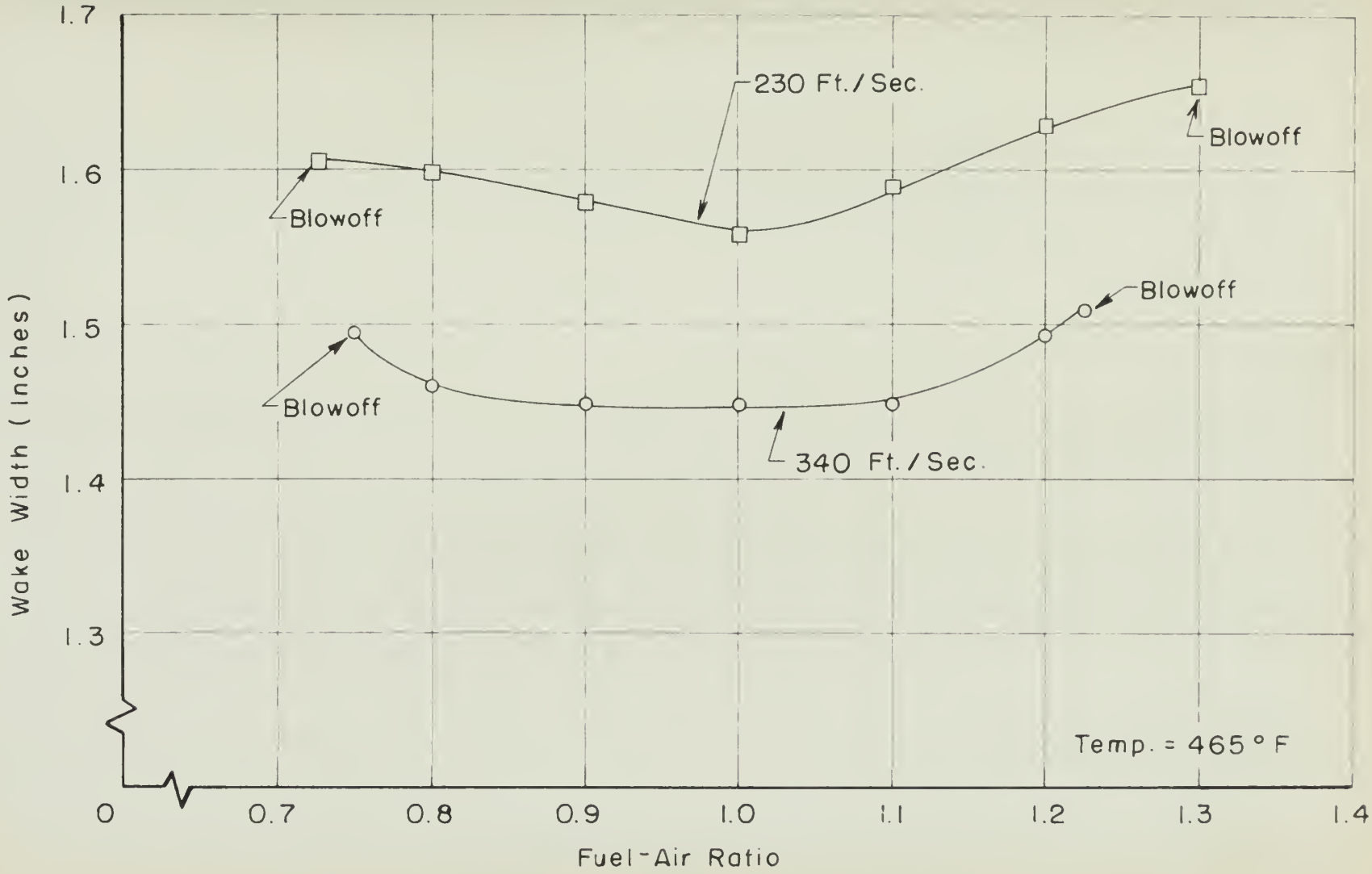


FIG.15-WAKE WIDTH AS A FUNCTION OF FUEL-AIR RATIO (FRACTION OF STOICHIOMETRIC) AT STATION 9" DOWNSTREAM OF FLAMEHOLDER

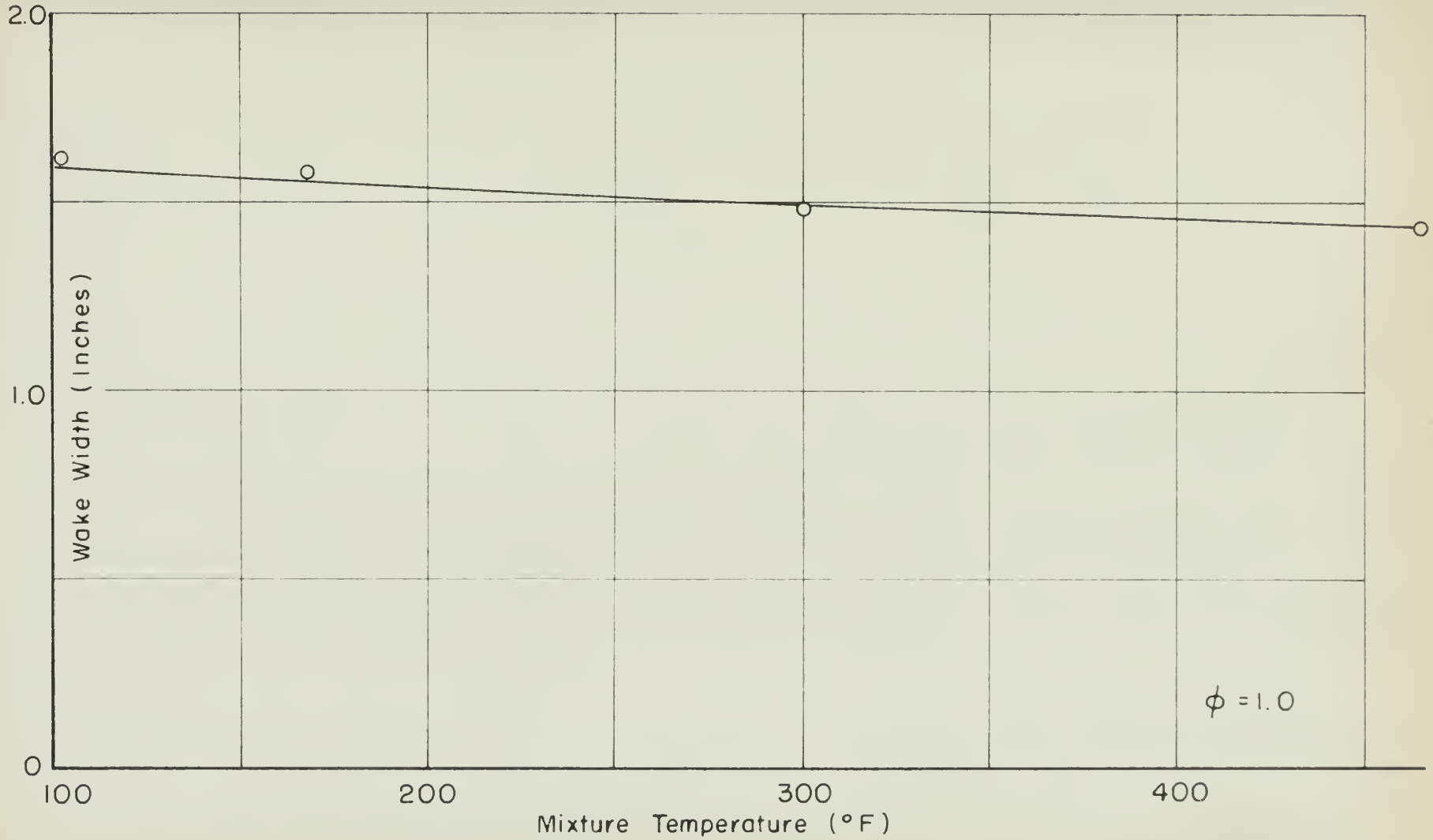




FIG. 16-WAKE WIDTHS ABOVE CRITICAL VELOCITY AS A FUNCTION OF TEMPERATURE 9" DOWNSTREAM OF FLAMEHOLDER

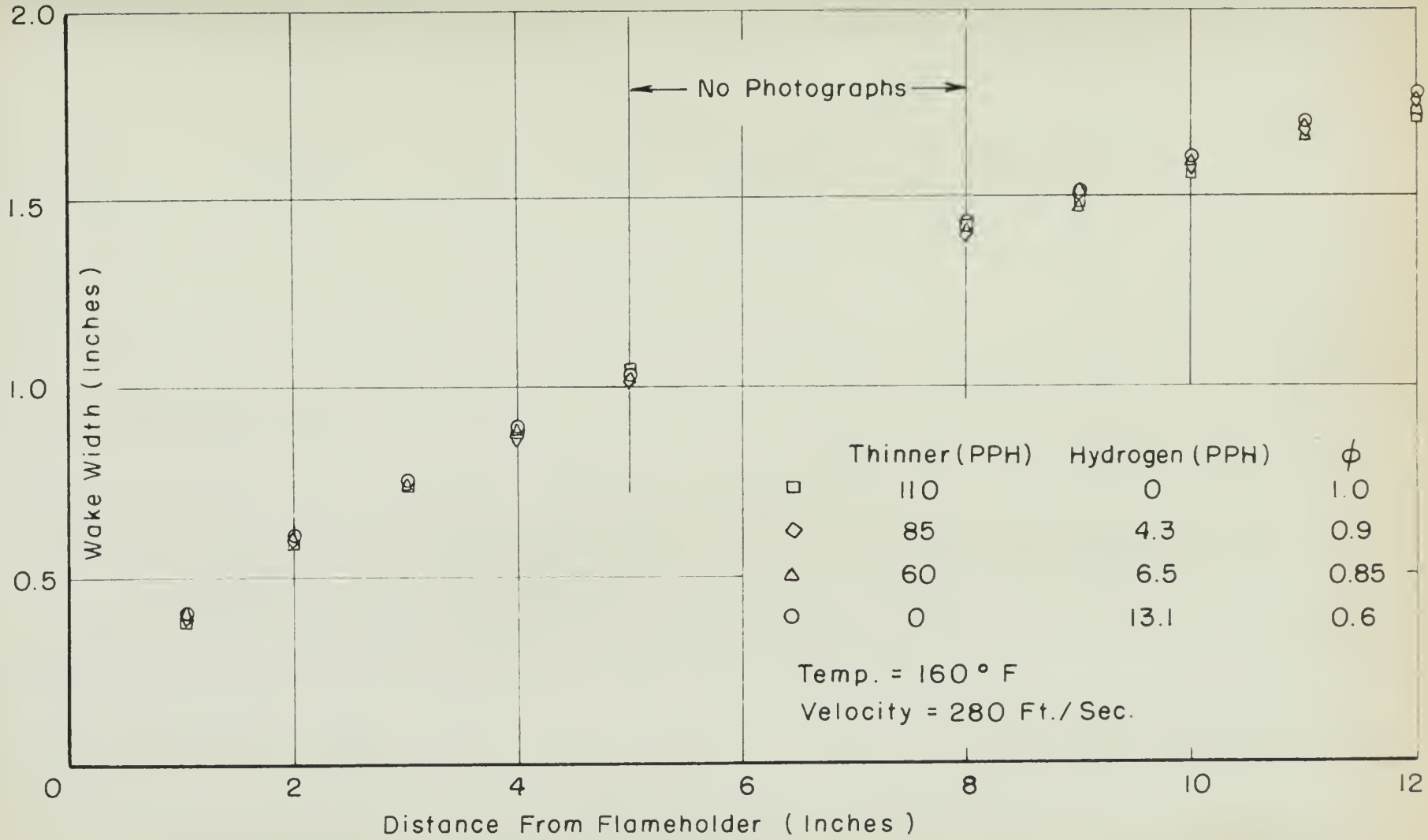


FIG. 17 - VARIATION OF WAKE WIDTH WITH FUEL COMPOSITION

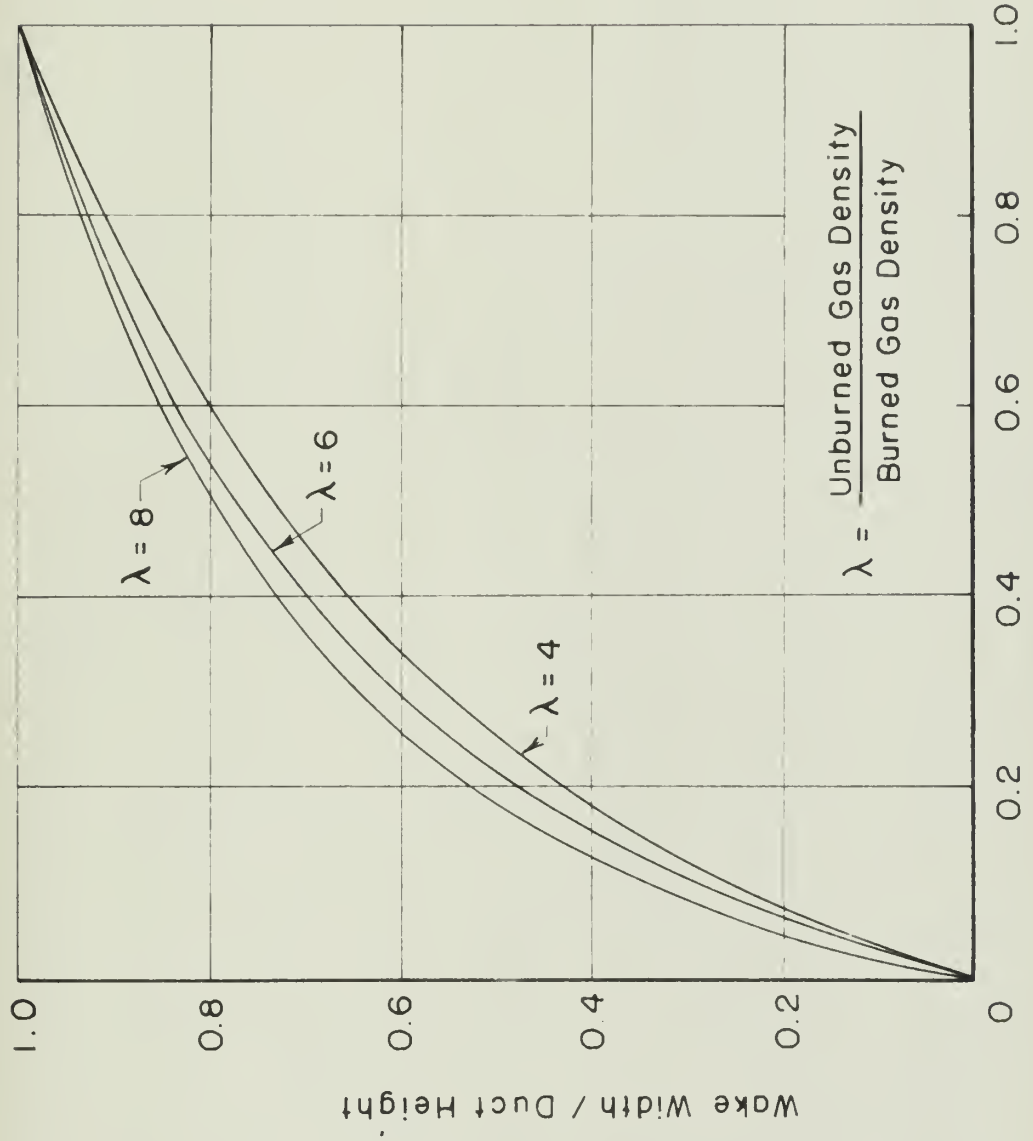


FIG. 18 - FLAME WIDTH AS A FUNCTION OF FRACTION BURNED
(Ref. "Influence Of Flame Front On The Flow Field, by H.S. Tsien")

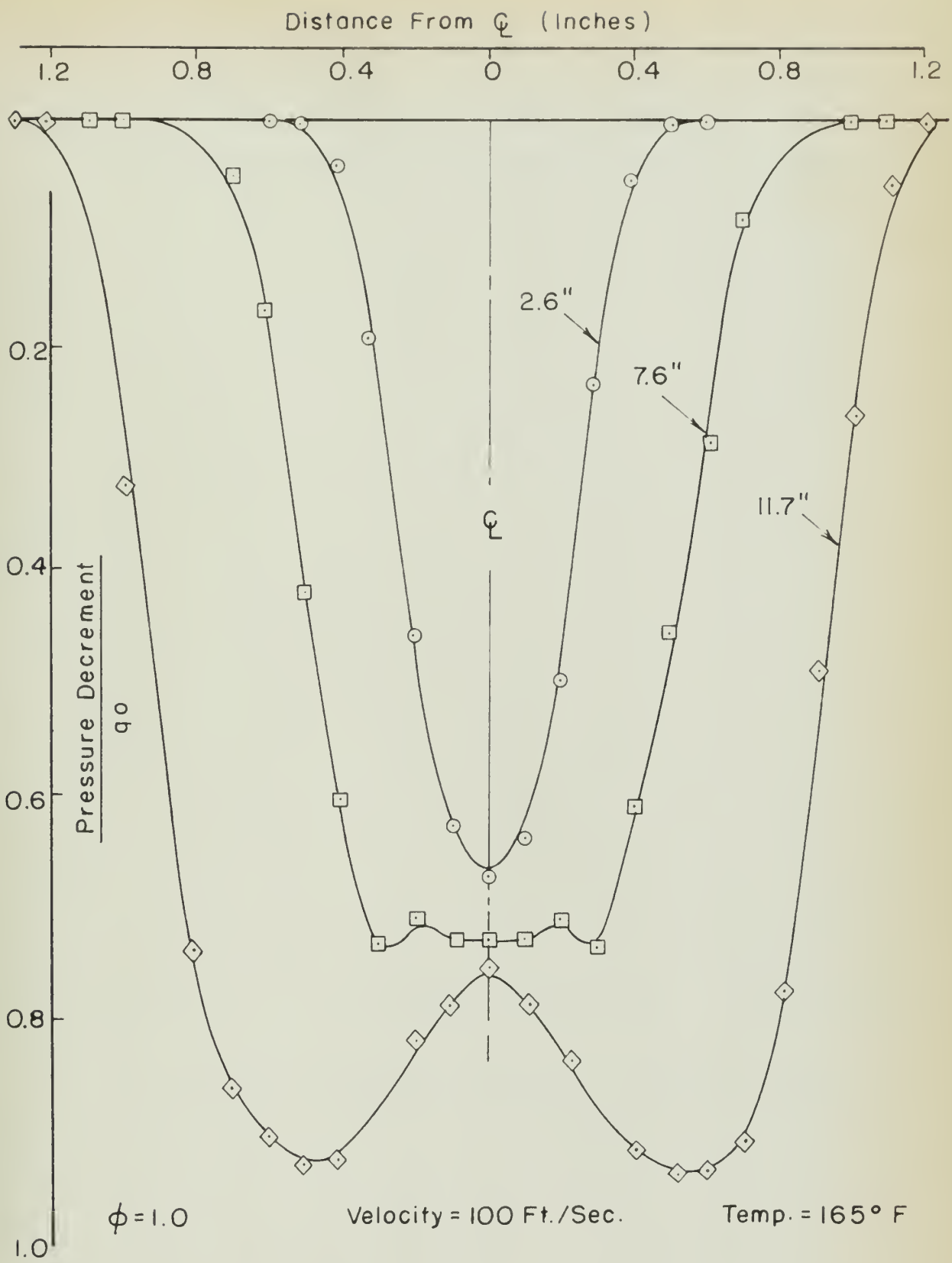


FIG. 19-PRESSURE PROFILES ACROSS FLAME

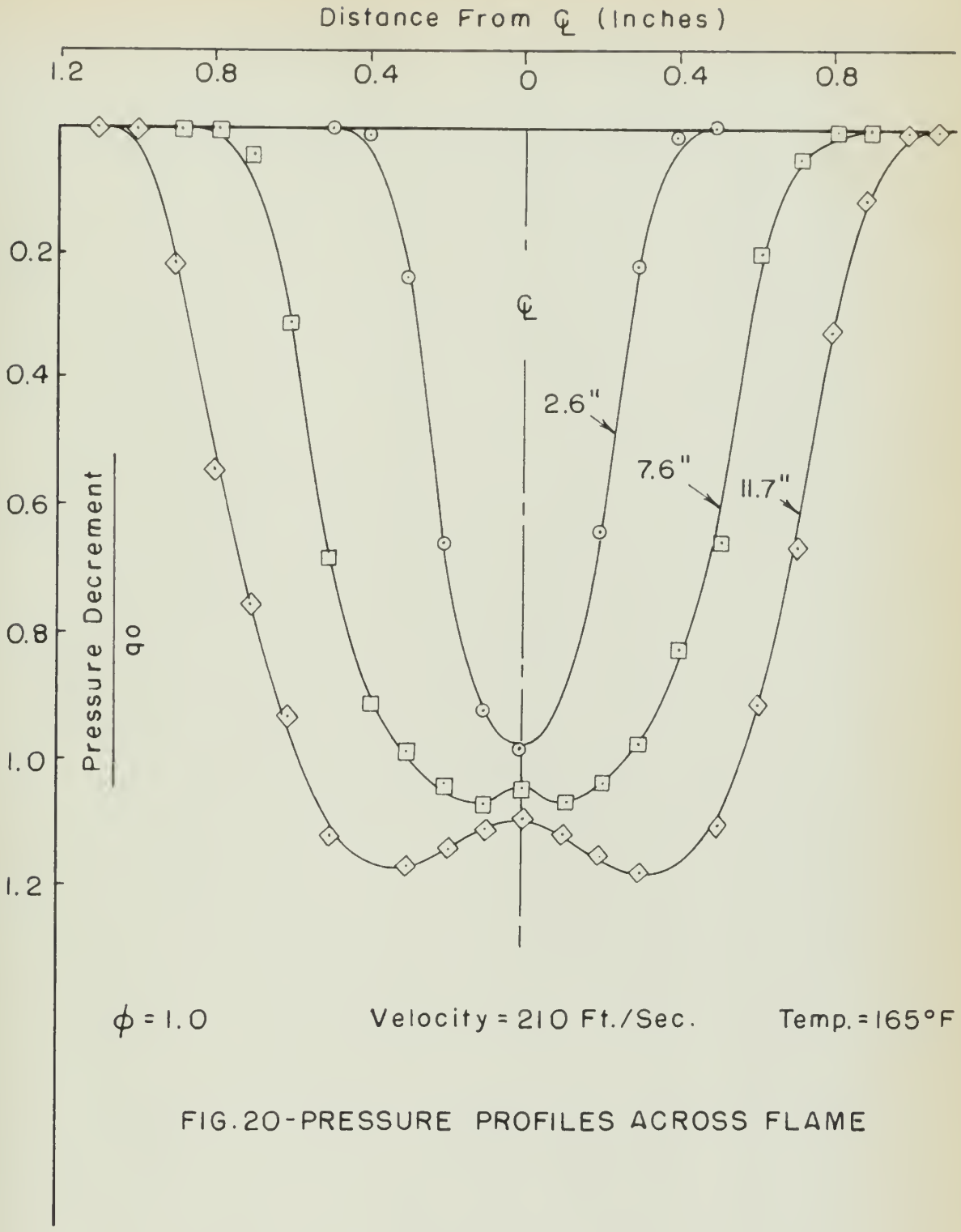


FIG. 20 - PRESSURE PROFILES ACROSS FLAME

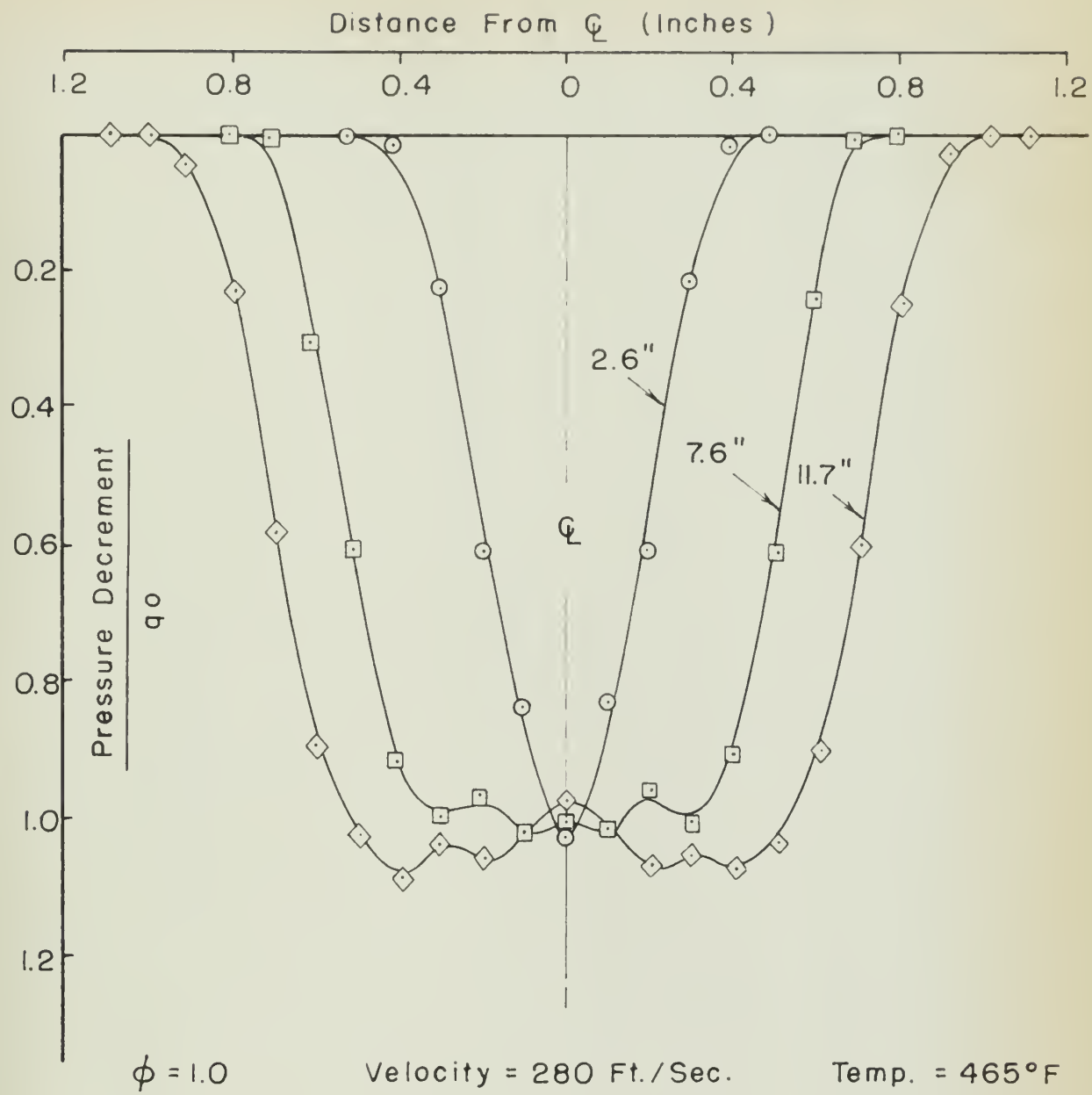


FIG. 21- PRESSURE PROFILES ACROSS FLAME

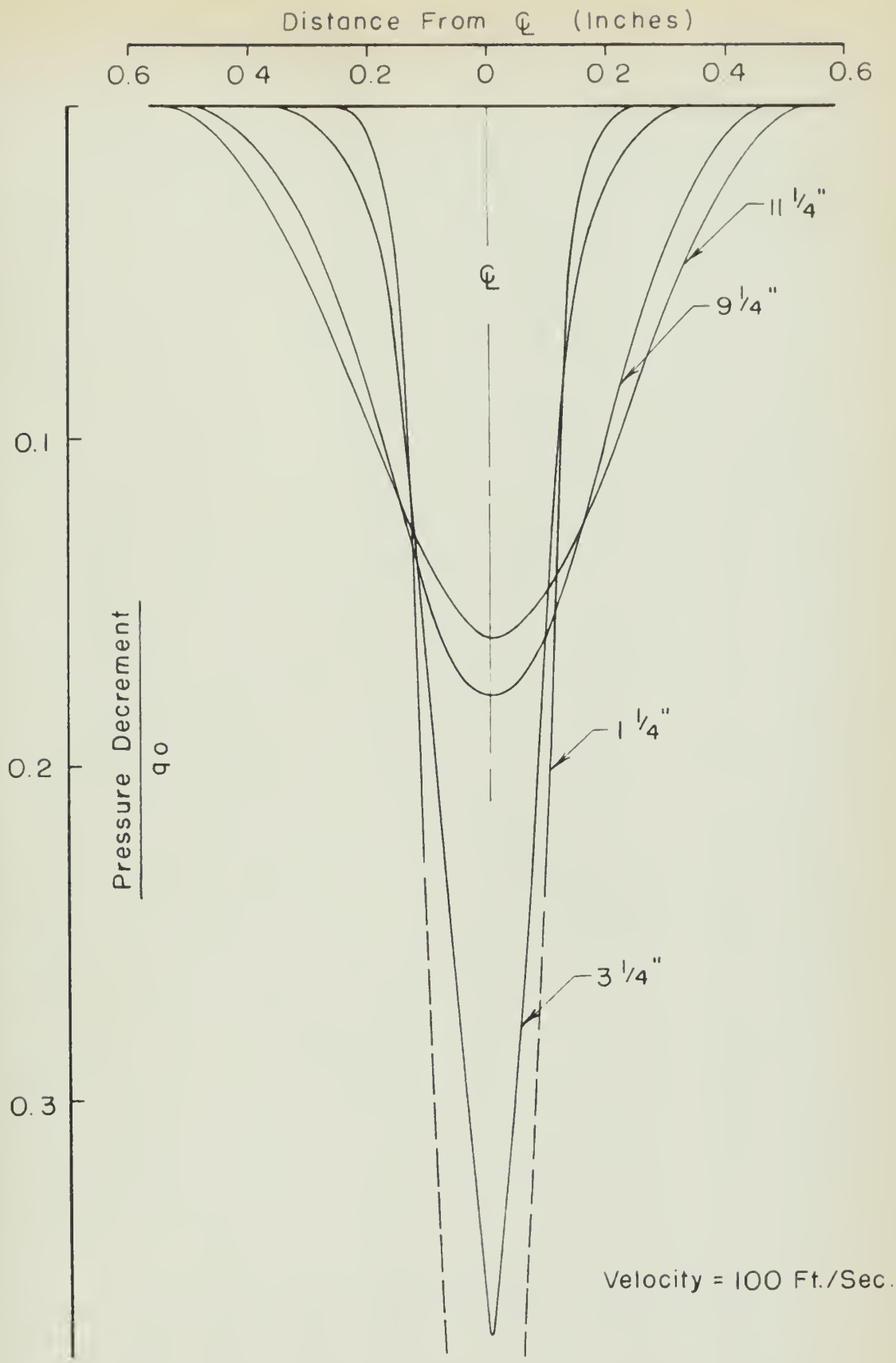


FIG.22-COLD FLOW PRESSURE PROFILES

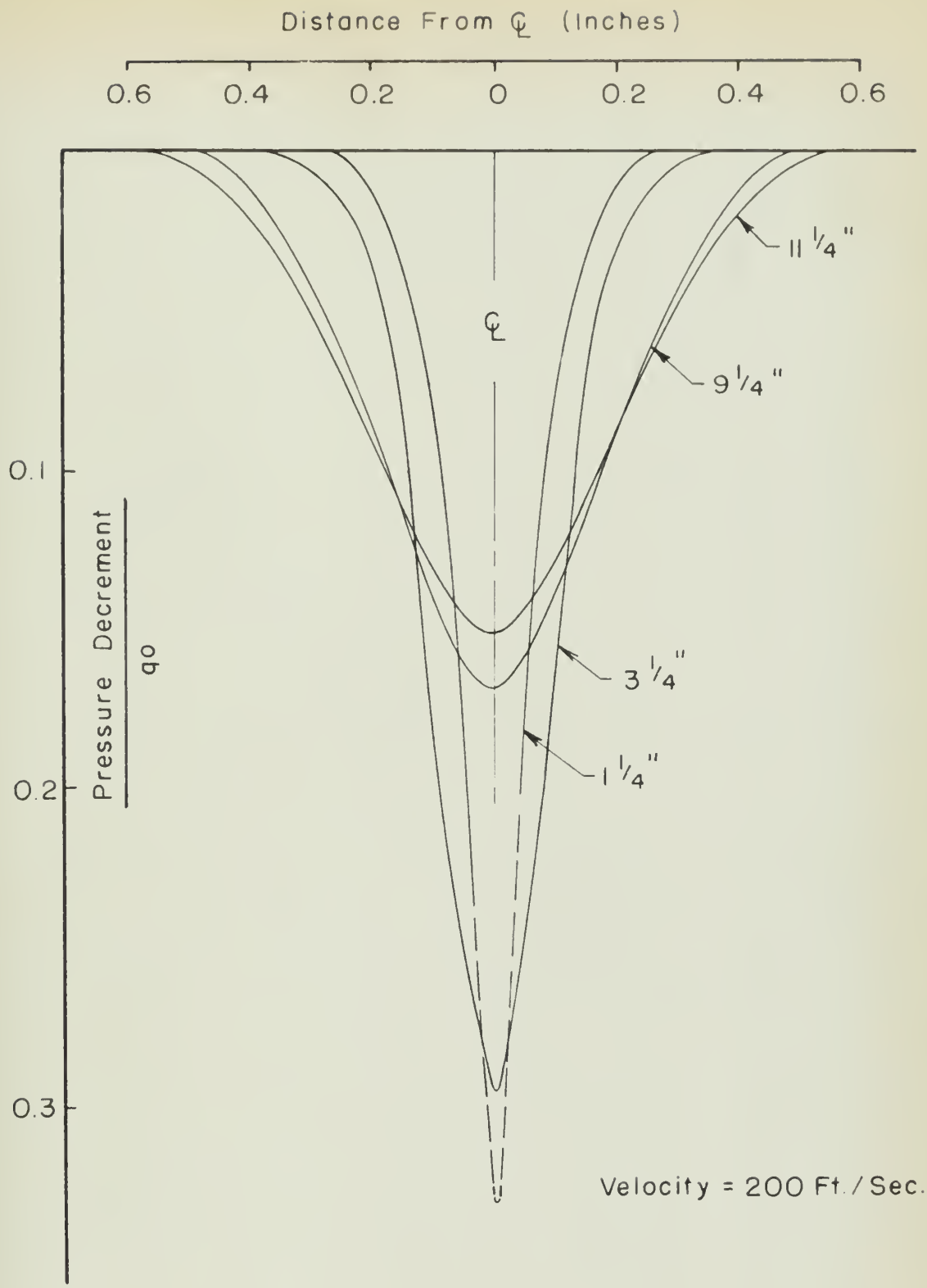


FIG.23-COLD FLOW PRESSURE PROFILES

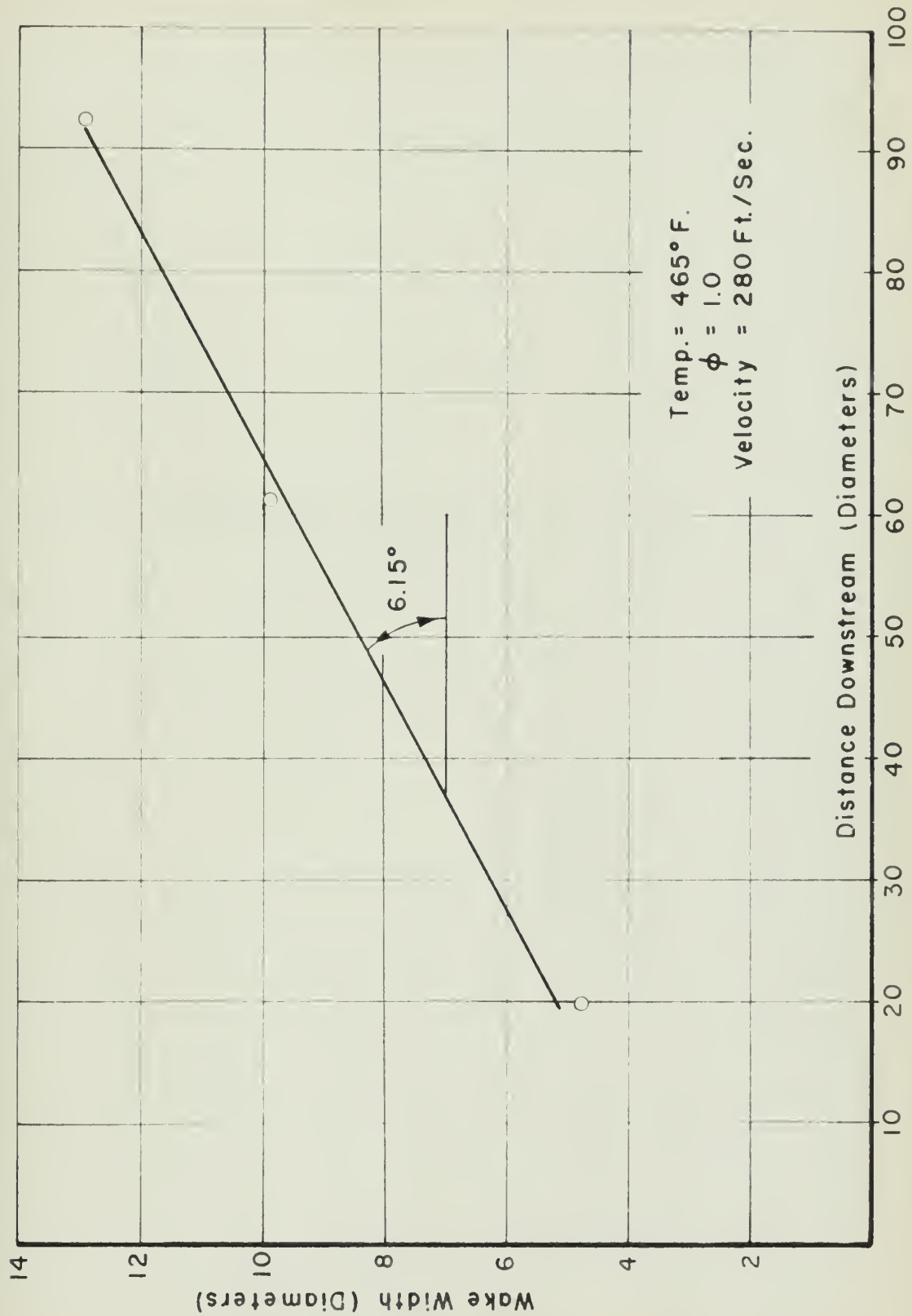


FIG.24- VARIATION OF WAKE WIDTH AT 20 PERCENT TOTAL PRESSURE DECREMENT WITH DOWNSTREAM DISTANCE

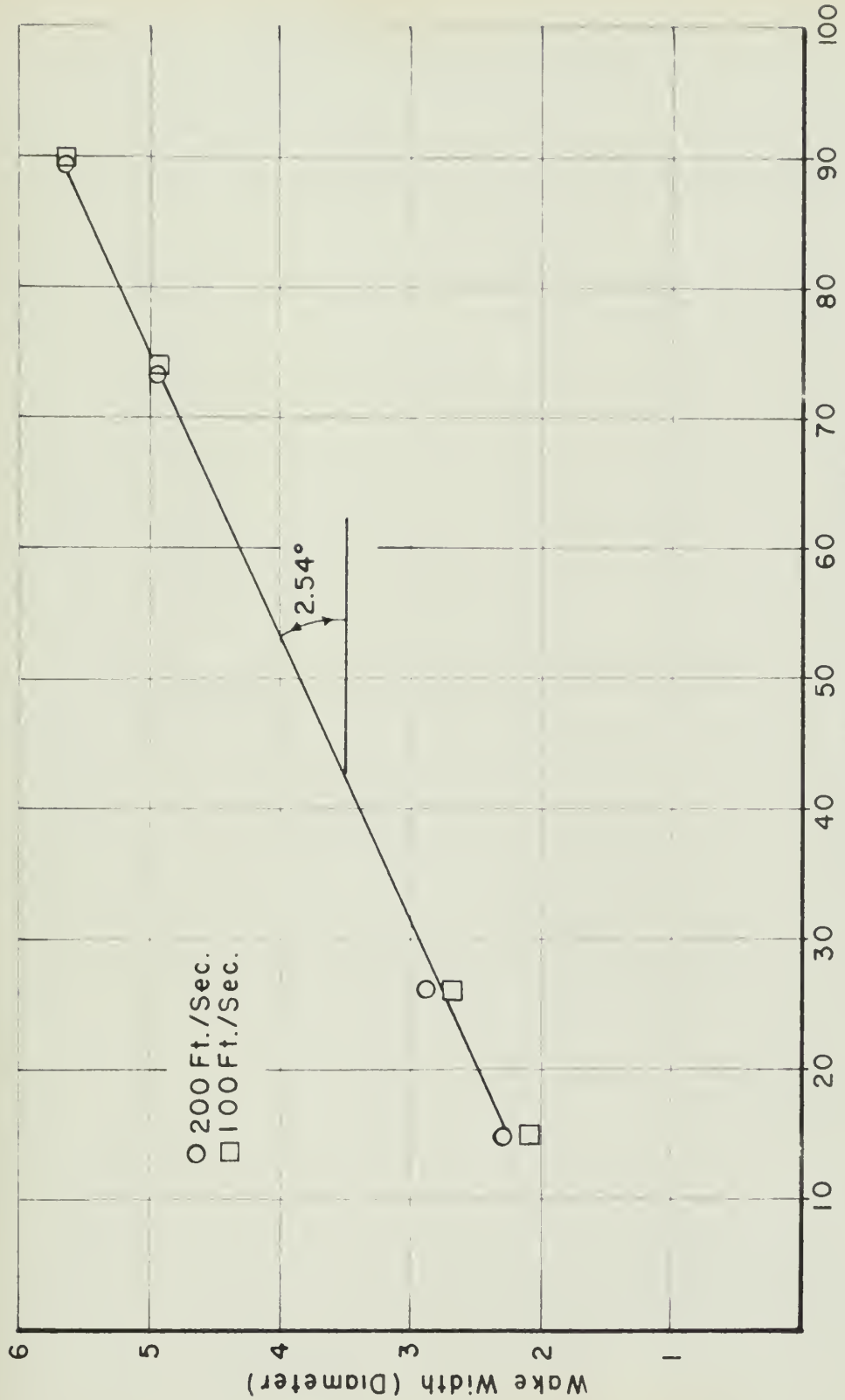


FIG. 25 - VARIATION OF WAKE WIDTH AT 20 PERCENT TOTAL PRESSURE DECREMENT WITH DOWNSTREAM DISTANCE. COLD FLOW

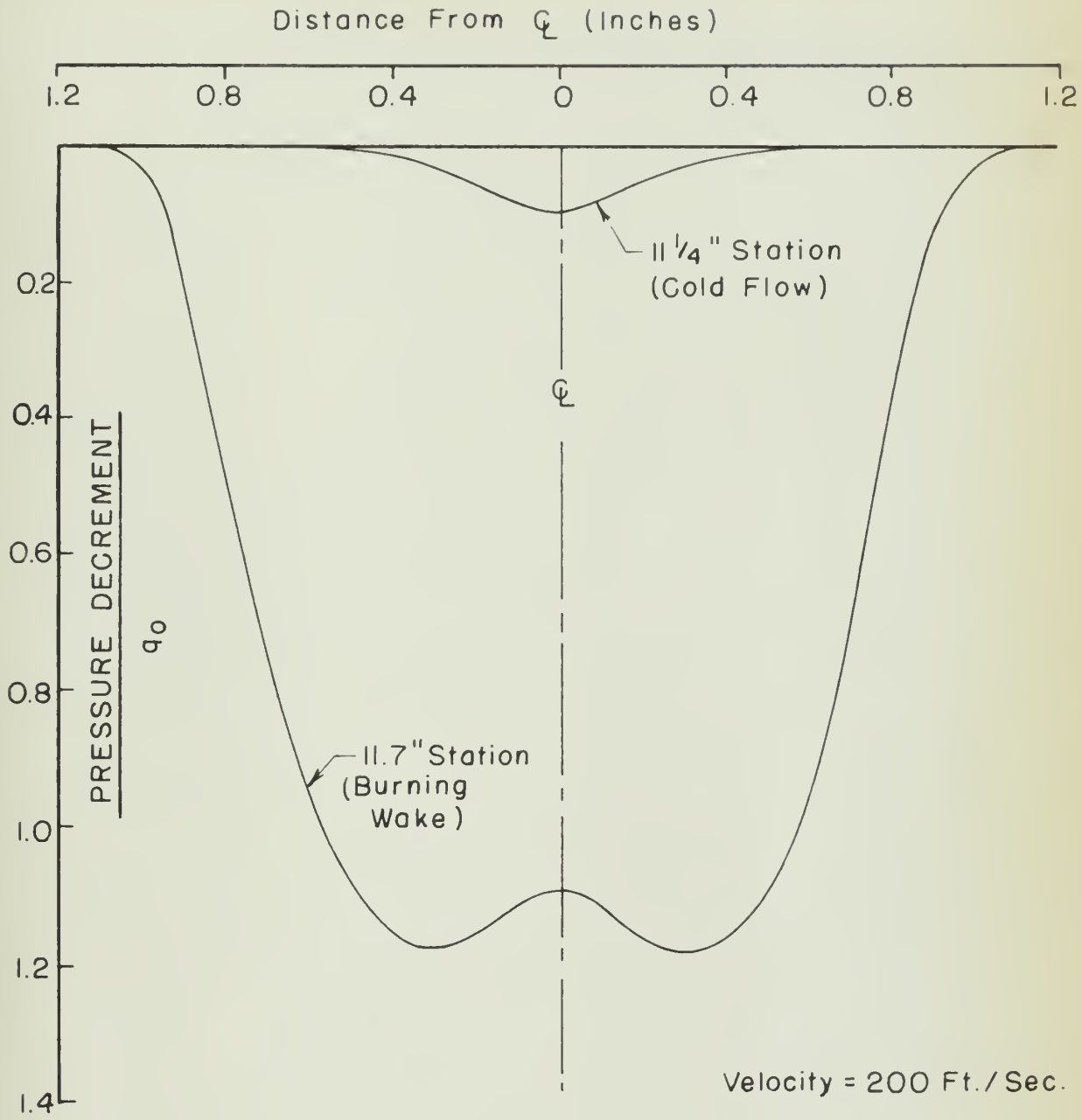


FIG. 26 - PRESSURE PROFILES OF BURNING WAKE AND COLD FLOW AT SAME VELOCITY AND SAME STATION